

**Simulating the Effects of Porosity and Permeability Variations to Optimize Coal Bed  
Methane Production**

by

Aderito Hilario Matevele

14167

Dissertation submitted in partial fulfilment of

the requirements for the

Degree of Study (Hons)

(Petroleum Engineering)

FYP II September 2014

Supervisor: Dr. Saleem Qadir Tunio

Universiti Teknologi PETRONAS

Bandar Seri Iskandar

31750 Tronoh

Perak Darul Ridzuan

CERTIFICATION OF APPROVAL

Simulating the Effects of Porosity and Permeability Variations to Optimization CBM Production

by

Aderito Hilario Matevele

This project dissertation submitted to the

Petroleum Engineering Department

Universiti Teknologi PETRONAS

in partial fulfilment of the requirement for the

BACHELOR OF ENGINEERING (Hons)

(PETROLEUM ENGINEERING)

Approved by,

---

(Dr. Saleem Qadir Tunio)

Universiti Teknologi PETRONAS

Tronoh, Perak

September 2014

## CERTIFICATION OF ORIGINALITY

This is to certify that I am responsible for the work submitted in this project, that the original work is my own except as specified in the references and acknowledgements, and that the original work contained herein have not been undertaken or done by unspecified sources or persons.

---

ADERITO HILARIO MATEVELE

## **ABSTRACT**

Coal bed methane (CBM) has become one of the most important future energy source in the world, along with other types of unconventional reservoirs such as shale gas and tight reservoirs. It is because of such discoveries that academic, oil and gas industry experts have started conducting studies and developing technologies to maximize recovery of methane adsorbed in coal.

Coal formations have low porosity and permeability, therefore, it is necessary to conduct studies to understand how to optimize natural gas recovery from coal. This project focuses on the effects of porosity and permeability with respect to production. Hydraulic fracturing stimulation technique is used in this paper to stimulate both the porosity and permeability of coal seam by injecting water into the formation. Thereafter, sensitivity analysis is conducted to study the effect of changing these two production control parameters to achieve CBM production optimization. The analysis are conducted based on hydraulic fracture models for coal seams, and to analyze the effects of porosity and permeability changes, Eclipse E300 is used. This research focuses on data from three distinct coal basins for analysis: Powder River, San Juan and Sarawak basins.

The results obtained indicate that coal formations are stimulated by injecting water into the formation at high rate and pressure. Results also show that by increasing permeability and porosity of coal, the production rate of natural gas is optimized.

## **ACKNOWLEDGEMENT**

First and foremost, I would like to express my endless gratitude to God Almighty for giving me strength and will to complete this Final Year Project dissertation. Without His blessings, I would surely not have had the required strength and motivation to proceed with my work.

Secondly, I am thankful to my supervisor, Dr. Saleem Qadir Tunio, for the time spent helping and supporting me throughout the whole project, and for his patience and guidance. His wide range of expertise, particularly in the Coal Bed Methane area, was fundamental for the successful execution of this project. Moreover, his constant motivation and advices were important encouragement tools for me to have strong determination attitude to do my work with the required level of professionalism. Despite his busy schedules he managed make time to guide and to answer my all questions.

Last but not least, my deepest thanks to my family and friends for the constant support and motivation to successfully complete this final year project dissertation.

# TABLE OF CONTENTS

|   |      |
|---|------|
| <b>ABSTRACT</b> .....   | iii  |
| <b>ACKNOWLEDGEMENT</b> .....  | iv   |
| <b>List of Figures</b> .....  | vi   |
| <b>List of Tables</b> .....   | vii  |
| <b>Nomenclature &amp; Abbreviations</b> .....                                   | viii |
| <b>CHAPTER 1: INTRODUCTION</b> .....  | 1    |
| <b>1.1 Background</b> .....   | 1    |
| <b>1.2 Problem Statement</b> .....  | 3    |
| <b>1.3 Objectives and Scope of Study</b> .....                                  | 3    |
| <b>CHAPTER 2: LITERATURE REVIEW</b> .....                                       | 4    |
| <b>2.1 Coal Geologic Properties</b> .....                                       | 4    |
| <b>2.1.1 Coal Rank</b> .....  | 4    |
| <b>2.2 Coal Reservoir versus Conventional reservoir</b> .....                   | 6    |
| <b>2.3 Porosity and Permeability Models</b> .....                               | 7    |
| <b>2.3.1 Porosity</b> .....   | 7    |
| <b>2.3.2 Permeability</b> .....   | 8    |
| <b>2.4 Classification of coal matrix pores and Gas-Water distribution</b> ..... | 11   |
| <b>2.5 Hydraulic Fracturing Mechanism</b> .....                                 | 11   |
| <b>2.5.1 Fracture Width Modeling</b> .....                                      | 13   |
| <b>2.5.2 Types of fracturing Fluids for Coal</b> .....                          | 14   |
| <b>CHAPTER 3: METHODOLOGY</b> .....   | 15   |
| <b>3.1 General Activities Flowchart</b> .....                                   | 16   |
| <b>3.2 General Project Milestones and Gantt chart</b> .....                     | 17   |
| <b>CHAPTER 4: RESULTS AND DISCUSSION</b> .....                                  | 18   |
| <b>4.1 Coal Flow Mechanism Analysis</b> .....                                   | 18   |
| <b>4.2 Hydraulic Fracturing Stimulation Results</b> .....                       | 19   |
| <b>4.3 Eclipse Simulation Results</b> .....                                     | 26   |
| <b>CHAPTER 5: CONCLUSION AND RECOMENDATIONS</b> .....                           | 35   |
| <b>5.1 Conclusion</b> .....   | 35   |
| <b>5.2 Recommendations</b> .....  | 36   |
| <b>References</b> .....   | 37   |

## List of Figures

|  |    |
|--|----|
| Figure 2.1: Types of pore spaces and the rock grains .....                               | 8  |
| Figure 2.2: Plan view of dual porosity cleat system of coal.....                         | 9  |
| Figure 2.3: Conceptual representation of coal/gas interactions.....                      | 10 |
| Figure 2.4: Effect of fracture on production rates.....                                  | 12 |
| Figure 2.5: Stress fracture orientations in coals.....                                   | 13 |
| Figure 3.1: Project's methodology steps.....   | 15 |
| Figure 3.2: General project activities flow.....   | 16 |
| Figure 4.1.1: Schematic analysis of flow mechanisms in coal.....                         | 18 |
| Figure 4.2.1: Determination of the injection permeability for the Powder River.....      | 20 |
| Figure 4.2.2: Fluid injection rate vs permeability change for Powder River.....          | 21 |
| Figure 4.2.3: Fluid injection rate vs porosity change for Powder River reservoir.....    | 21 |
| Figure 4.2.4: Determination of the injection permeability for the San Juan.....          | 22 |
| Figure 4.2.5: Fluid injection rate vs permeability change for San Juan reservoir.....    | 23 |
| Figure 4.2.6: Fluid injection rate vs permeability change for San Juan reservoir.....    | 23 |
| Figure 4.2.7: Determination of the injection permeability for the Sarawak reservoir..... | 24 |
| Figure 4.2.8: Fluid injection rate vs permeability change for Sarawak reservoir.....     | 25 |
| Figure 4.2.9: Fluid injection rate vs permeability change for Sarawak reservoir.....     | 25 |
| Figure 4.3.1: Field gas production due to permeability variations (Powder River).....    | 26 |
| Figure 4.3.2: Field gas production due to porosity variations (Powder River).....        | 27 |
| Figure 4.3.1: Field gas production due to permeability variations (San Juan).....        | 28 |
| Figure 4.3.1: Field gas production due to porosity variations (San Juan).....            | 28 |
| Figure 4.3.1: Field gas production due to permeability variations (Sarawak).....         | 29 |
| Figure 4.3.1: Field gas production due to porosity variations (Sarawak).....             | 30 |

## List of Tables

|  |    |
|--|----|
| Table 1.1: Worldwide geographic distribution of coal bed gas by original gas in place..... | 2  |
| Table 2.1: ASTM coal ranks.....  | 5  |
| Table 2.2: Life time of the CBM field vs Conventional reservoirs.....                      | 7  |
| Table 2.3: Types of fracture fluids in coal.....   | 14 |
| Table 3.1: Project activities and deadlines.....   | 17 |
| Table 3.2: FYP 2 project activities and key milestones.....                                | 17 |
| Table 4.1: Analysis of the effect of permeability and porosity on production.....          | 31 |
| Appendix A: Table of Coal matrix pores classification table by various authors.....        | 39 |
| Appendix B: Coal properties of Powder River Basin, San Juan and Sarawak.....               | 40 |



## Nomenclature & Abbreviations

**CBM** – Coal bed methane

**OGIP** – Original gas in place

**TCF** – Trillion cubic feet

**G<sub>s</sub>** - Gas storage capacity (SFC/ton)

**V<sub>L</sub>**- Langmuir's volume constant (SFCc/ton)

**P<sub>L</sub>**- Langmuir's pressure constant (psia)

**P**- Formation pressure (psia)

$\phi_f$  – Fractured porosity

$\nabla^2$ - Laplacian operator

$c_f$  – Fracture compressibility

**t** –Time

$X_f$  - Position

$k_f$ - Fracture permeability of the formation

$\mu$  -Fluid viscosity

$\epsilon$  - Strain

**E** – Young's modulus

$\nu$  – Poisson's ratio

$\sigma_3$  - Vertical stress

$\sigma_1$  – Pressure causing deformation

$\sigma_2$  – Maximum horizontal in-situ stress

**K** - Permeability after injection

**Q<sub>inj</sub>** - Injection rate

**r** –Wellbore radius

**r<sub>e</sub>**- Drainage area

**K<sub>o</sub>** - initial coal permeability

# CHAPTER 1: INTRODUCTION

## 1.1 Background

The term CBM stands for coal bed methane, which is understood as natural gas produced from coal beds. The natural gas in the coal matrix is formed during coalification process and trapped within and adsorbed to the coal surface. CBM gas can also be called sweet gas due to lack of hydrogen sulfide (Chase, 1977).

Coal bed methane has distinct properties compared to those of a typical sandstone or other conventional gas reservoir given that methane is stored within the coal by a process called adsorption. The presence of this gas is well known from its occurrence in underground coal mining, where it presents a serious safety risk. Methane was traditionally extracted from coal mines to reduce hazards associated with the mining activity. The process consisted of dispersing the produced gas to the atmosphere. Methane gas capacity to flow through and be produced from coal seam is related to the permeability of the coal seam (Chen et.al, 2013)

Furthermore, the permeability of coal reservoirs is related to the porosity of the coal (cleats and pore spaces). The cleat formations is generally caused and affected by tectonic movements and the coalification process under high pressure and temperature. Face cleats are continuous, and form pathways of higher permeability than the discontinuous butt cleats (Dart Energy, 2013). The natural gas produced from coal bed fields contains predominantly methane and contain as well small percentages of ethane, propane, CO<sub>2</sub>, propane but does not contain liquid hydrocarbons (Chen et.al,2013).

Hassim (2012), indicates that the production of gas from coal beds all over the world is estimated to be around 256 trillion cubic meters in total. Recovering about one half of the world coal bed total resources would result in a global increase of natural gas reserves by 128 billion cubic meters, which represents a gain of about two thirds.

The largest coal bed resources are found in North America, Austral-Asia, and in the Commonwealth Independent States, however most of the resources remain yet to be recovered due to lack of technology and incentives in some countries (Dong et.al, 2009).

Table 1.1: Worldwide geographic distribution of coal bed gas by original gas in place

Source: (Dong et.al, 2005)

| <b>Region</b>                   | <b>Estimated OGIP: year<br/>1997 (TCF)</b> | <b>Estimated OGIP: year<br/>2012 (TCF)</b> |
|---------------------------------|--|--|
| Austral – Asia                  | 1,724                                      | 1,348                                      |
| North America                   | 3,017                                      | 1,629                                      |
| Commonwealth Independent States | 3,957                                      | 859  |
| Latin America                   | 39   | 13   |
| Middle East                     | 0  | 9  |
| Europe                          | 274  | 176  |
| Africa                          | 39   | 18   |

The US and western Canada are estimated to have a total volume of original coal bed gas in place of over 1,763 to 2,343 trillion cubic feet, for a total of 16 sedimentary basins including Alaska (Dong, Holditch, Ayers, & Lee).

Since the discovery of the potential of CBM fields, many studies have been conducted on various mechanisms to optimize the recoverable gas from coal beds over the past years. The base of this studies focused mainly in analyzing the geological properties of coal, especially the porosity and permeability which play a major role in the hydrocarbon production. Since coal has low porosity and permeability, various methods have been introduced in the industry with the main objective of maximizing the coal productivity by increasing the porosity and permeability.

## **1.2 Problem Statement**

One of the most important factor to successfully optimize natural gas production from coal formations is to understand the reservoir properties of the coal. Unlike conventional natural gas reservoirs, CBM reservoirs have low porosity and permeability. This means that the pore spaces or void spaces between the matrices of the coal formation are very small and tight, with very small interconnected channels through which fluids can flow to the production stream.

So, there is a need of conducting sensitivity analysis to understand how much variations of permeability and porosity due to hydraulic fracturing can affect the productivity of coal beds in order to optimize natural gas production.

## **1.3 Objectives and Scope of Study**

The objectives of this study are:

- To simulate porosity and permeability variation by hydraulic fracturing in coal beds.
- To investigate the effect of the variation of permeability for CBM optimization by conducting sensitivity analysis.
- To investigate the effect of the variation of porosity for CBM optimization by conducting sensitivity analysis.

The research will focus mainly on the stimulation of reservoir properties controlling CBM production (permeability and porosity) of three CBM fields in order to study how much these two parameters can influence the production optimization of CBM.

## **CHAPTER 2: LITERATURE REVIEW**

The search for hydrocarbons over the recent years has been a great challenge in the oil and gas industry. With the population growth, the demand of energy source has increased exponentially hence forcing industry experts to search for new sustainable sources of energy. It is because of such factors and many others that unconventional fields became the focus of oil and gas exploration. Coal bed methane is the object this study.

Unlike conventional reservoirs, coal is the source, trap, and reservoir. Comparing the two reservoir types shows profound differences in reservoir properties, storage mechanisms, drive mechanisms, and production profile. Gas contained in coal bed methane is mainly methane and trace quantities of ethane, nitrogen, carbon dioxide and few other gases. Intrinsic properties of coal as found in nature determine the amount of gas that can be recovered (Chen et.al, 2013).

### **2.1 Coal Geologic Properties**

According to Hassim (2012) coal beds have distinct geologic properties, related to the origin and formation processes of each coal over time. Coal can be classified according to the coal ranks, coal types and grade.

#### **2.1.1 Coal Rank**

Another concept which is relevant to understand CBM is the coal rank. It can be described as the measure of the quality and thermal maturity of the organic matter. Coal passes through four classes in its maturation: lignite, subbituminous, bituminous, and anthracite (Materials, 1998).

The coalification process is due to the alteration a variety of chemical, mechanical and biological mechanisms that occurred over time.

Coal rank is usually assessed by series of tests known as proximate analysis. Furthermore, the test helps obtaining the moisture content, fixed carbon, volatile mater, ash content, calorific value and the fixed sulfur content.

The American Society for Testing and Materials (ASTM) established a table of coal ranks classification indicated in table 2.1. The recognition of coal ranks is important because it provides insight into the coal strength, water sensitivity, density, surface area and permeability which are of massive use in the CBM production optimization studies (Barr, 2009).

Table 2.1: ASTM coal ranks. *Source:Materials (1998)*

| <b>ASTM coal rank classes</b>   | <b>Rank categories</b>  |
|---|-------------------------|
| Peat  | Peat (low Rank)         |
| Lignite A<br>Lignite B<br>Sub Bituminous A, B and C<br>High Volatile Bituminous C                                 | Lignite                 |
| High Volatile Bituminous B<br>High Volatile Bituminous A<br>Medium Volatile Bituminous<br>Low Volatile Bituminous | Bituminous              |
| Semi - Anthracite<br>Anthracite<br>Meta – Anthracite  | Anthracite ( High rank) |

## 2.2 Coal Reservoir versus Conventional reservoir

According to (Ramachandran & Shirley, 1994) natural gas components deposits, such as the lower molecular weight hydrocarbons, found in the underground coal formations occur due to the effects of long term coalification process. The coal normally has low porosity and permeability compared to conventional reservoirs, therefore the natural gas is mostly in form of sorbate on the surfaces of the coal.

The storage process of the natural gas in the coal is completely different from conventional gas reservoirs: gas does not occupy the void spaces as free gas between the grains (conventional reservoirs), whereas the gas in coal, is held to the solid surface of the coal by adsorption in numerous micro pores of the coal matrix.

The production of methane from coal is related to the pressure depletion due to dewatering process. The Langmuir's equation is used to determine the amount of methane adsorbed in coal formations (Hassim, 2012).

$$G_s = \frac{V_L P}{P_L + P} \quad (\text{Eq.1})$$

Mass transport mechanism in coal depends on the methane concentration gradient not in the pressure gradient like in the conventional reservoirs. Coal is the source, reservoir and the sealing rock (Ramachandran & Shirley, 1994).

For further understanding of how CBM reservoirs differs from the conventional natural gas reservoirs in terms of the production behavior within the life time of the fields, table 2.2 analyzing three production stages is generated: at the beginning, middle life time, and at the end of the reservoir life time.

Table 2.2: Life time of the CBM field vs Conventional reservoirs; *Source (Purl, Evanoff, & Brugler, 1991).*

| Coal Seam/CBM   | Conventional Reservoir   |
|---|--|
| <ul style="list-style-type: none"> <li>▪ Dewatering takes place in the initial phase and the gas rate is very low.</li> <li>▪ Methane gas migrates to the coal cleats and to the well as the reservoir pressure declines.</li> <li>▪ Natural gas production tends to increase before beginning to decline.</li> </ul> | <ul style="list-style-type: none"> <li>▪ At the beginning, maximum gas rate is observed and the pressure is very high.</li> <li>▪ As pressure declines with time, the production rate also declines.</li> <li>▪ Water production increases, inhibiting hydrocarbon production</li> </ul> |

## 2.3 Porosity and Permeability Models

### 2.3.1 Porosity

According to Jon Gluyas (2004), porosity can be defined as the total volume of void space in the rock, including pores, vugs, and fractures. It can as well be defined as the ratio of the total void volume to the bulk volume. It is expressed as a fraction or percentage. Not all pores are alike: there are big pores and little pores, pores with simple shapes, and others with highly complex 3D morphologies. Knowledge of the size and shape of pores and the way in which they are interconnected is important, because these factors that will determine the permeability of the rock (Jon Gluyas, 2004). In coal formations, porosity is estimated to range from 0.1 to 10% in general(Wikipedia, 2010). Figure 2.1 below shows the types of pore spaces of coal seams. From the figure three types of pores are represented: dead end pores, isolated pores and the interconnected pores.



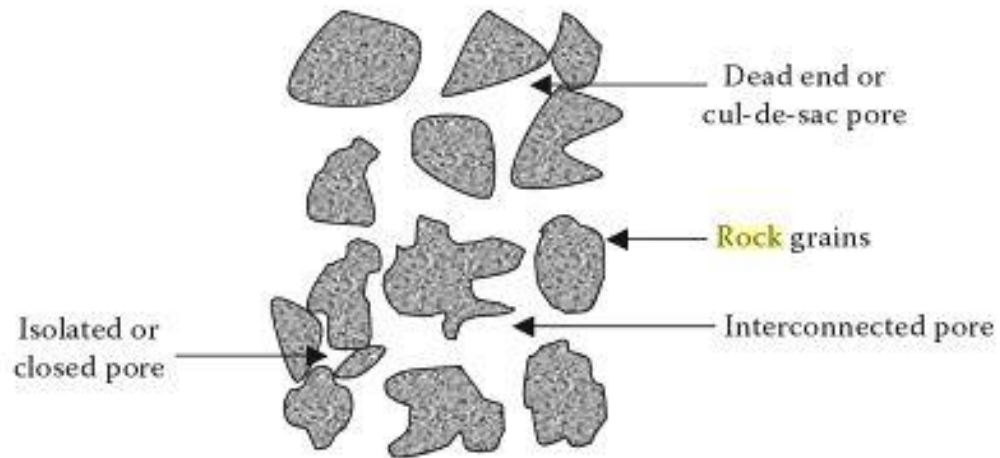


Figure 2.1: Types of pore spaces and the rock grains: *Source: (Djebbar Tiab, 2004).*

### 2.3.2 Permeability

Apart from being porous, a reservoir must have the capacity to allow fluids to move through the interconnected pore spaces. This ability that the reservoir rock have to conduct fluids is referred to as Permeability. The permeability of a rock depends on the effective porosity, hence, it is affected by the rock's grain shape, size and distribution, as well as the grain packing and the degree of consolidation and cementation (Djebbar Tiab, 2004). Moreover, Jon Gluyas (2004) also defines permeability is the intrinsic property of rocks that determines how easily a fluid can flow through the reservoir. The permeability of coal formations is relatively small compared to conventional reservoirs, ranging from 0.1–50 milliDarcies depending on different locations (Jochen & Lee, 1994).

Due to the presence of face and butt cleats on coal reservoirs, Coal bed methane reservoirs are considered to be fractured naturally. The face cleats are continuous throughout the seam, while butt cleats are short and discontinuous. They usually align orthogonal to each other. In general, it can be assumed that the maximum permeability direction align parallel to the direction of face cleats (Chaianansutcharit, Chen, & Teufel, 2001).

According to (Z. Chen, Liu, Kabir, Wang, & Pan, 2013) two models control the productivity of CBM: the dual porosity model and the dual permeability model. Coal formations are characterized by the dual porosity model. This model assumes that natural gas is stored in the coal matrix and flow occurs only in fractures. Studies have been conducted but it is assumed that the gas transport mechanism is a diffusion process (Z. Chen et al., 2013). The dual permeability model on the contrary, represents the both the porosity and permeability of all the components: matrix/matrix, matrix/fracture, and fracture/fracture connections. Dual permeability model has been incorporated to represent the permeability response in deforming formations, to accommodate gas flow, and to evaluate the response to geo-mechanical influences (Z. Chen et al., 2013).

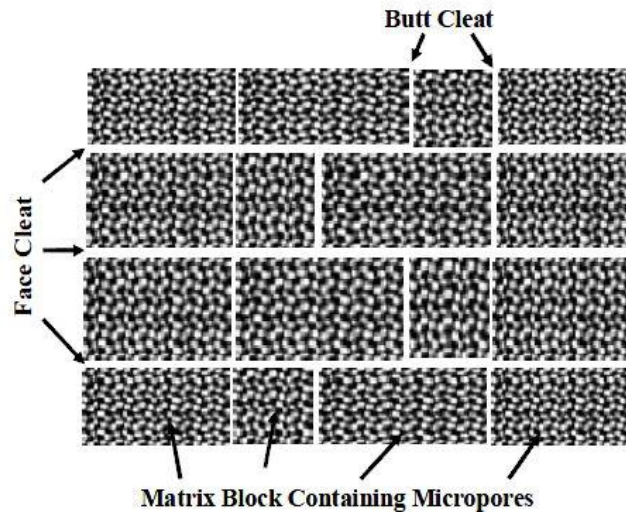


Figure 2.2: Plan view of dual-porosity cleat system of coal: *Source* :(Z. Chen et al., 2013)

The dual porosity equation for flow is shown below according to (Connell & Lu, 2007):

$$\frac{\phi_f \mu c_f}{k_f} \frac{dP(t, X_f)}{dt} - \nabla^2 P(t, X_f) = \frac{\mu_f}{\rho k_f} Q(t, X_f) \quad (\text{Eq.2})$$

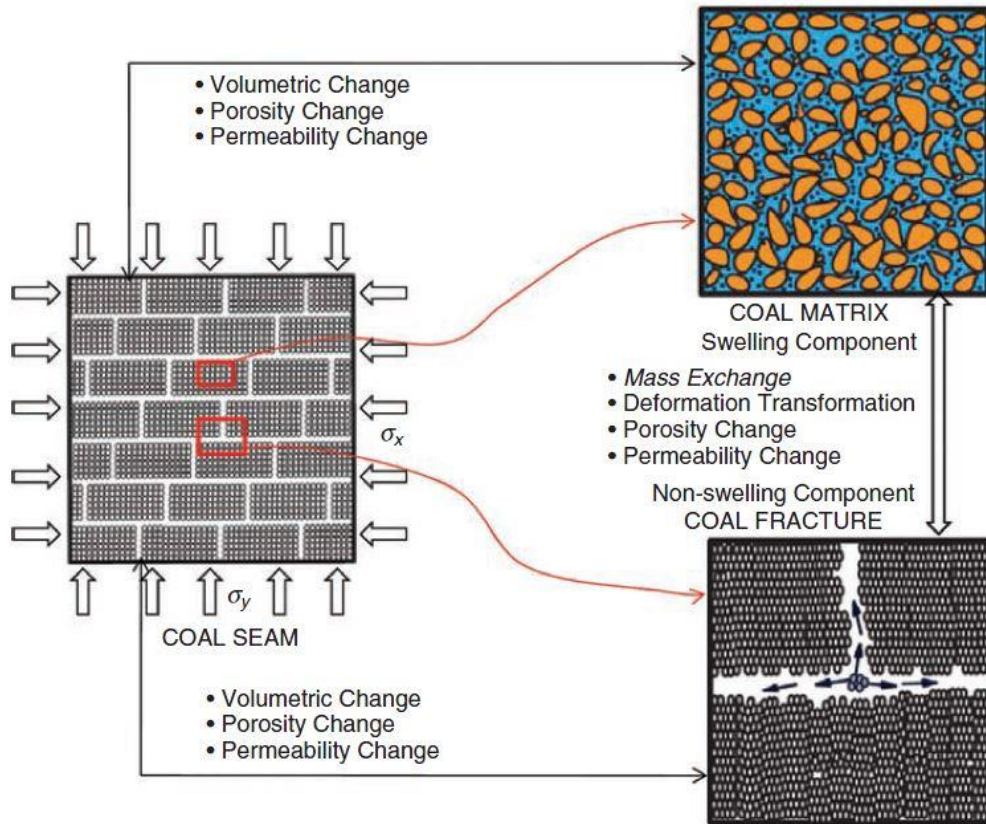


Figure 2.3: Conceptual representation of coal/gas interactions. *Source: (Z. Chen et al., 2013)*

Figure 2.3, coal - gas interactions in the coal seam are represented. It can be observed that the dewatering process enables the coal to undergo deformation, causing the coal to fracture. The fracture will then result in permeability and porosity change of the coal matrix.

Coal cleat system represents the permeability. As the coal rank increases cleat system also increases (Barr, 2009). According to (D. Chen, Liu, Pan, & Connell) many permeability models have been proposed, under two distinct effects of sorption – induced volumetric strain and stress – induced volumetric strain to predict permeability evolution. Furthermore, studies conducted indicate that the ratio of permeability of face to butt cleats can vary from 0 to 17 and the volumetric strain permeability model could not be applicable to the permeability anisotropy of coal.

## **2.4 Classification of coal matrix pores and Gas-Water distribution**

A research conducted by Ren et al. (2013) states that coal matrix must first be understood in order to better investigate the desorption and transport system of coal seams. Other researches by different authors present distinct methods of classification of coal (Ren et al., 2013). A general table of the classifications is presented in the appendix A for reference.

According to (Ren et al., 2013) the water in the coal pores and cleat system of CBM reservoirs is initially in a continuous phase, containing dissolved gas. Moreover, gas adsorbs in the internal surface of coal pores for the middle and high rank coals. The gas accounts for 80 to 90 % of all gases while the other 8 to 12% is the free gas, and dissolved gas accounts for about 1% (Ren et al., 2013). For low rank coal (peat), matrix pores are larger than those of middle and high rank coals (Lignite and Bituminous), therefore the ratio of free gas is higher compared to the other two coal ranks (Ren et al., 2013). This is due to:

- Coalification extent.
- Coal quality.
- Water saturation.

## **2.5 Hydraulic Fracturing Mechanism**

In order to increase the productivity of certain well, petroleum industry experts use a process designated as hydraulic fracturing. In open hole completion, hydraulic fracturing is conducted by sealing off the well in one section, and injecting fluids at high pressure until the formation fractures, resulting in improvement of the permeability (Haimson & Fairhurst, 1969). Hydraulic fracturing is conducted following certain assumptions such as: brittle formation, homogeneous, isotropic, the fluid flow obeys Darcy's law, linearly elastic formation, porous and that the exerted stress acts vertically parallel to the wellbore (Haimson & Fairhurst, 1969).

Production optimization by hydraulic fracture in coal seams have received mixed reviews. Studies conducted by Mavko, Hanson, Nielsen, and Logan (1986), concluded that the fractures tend to be shorter with large apertures and the vertical fractures propagate into the upper boundary of the rocks.

The hydraulic fracturing models currently in use in the industry employ two – dimensional fracture descriptions and follow the principle of mass conservation. These models do not specify what parameters control the propagation and to what distance it will propagate (Mavko et al., 1986).

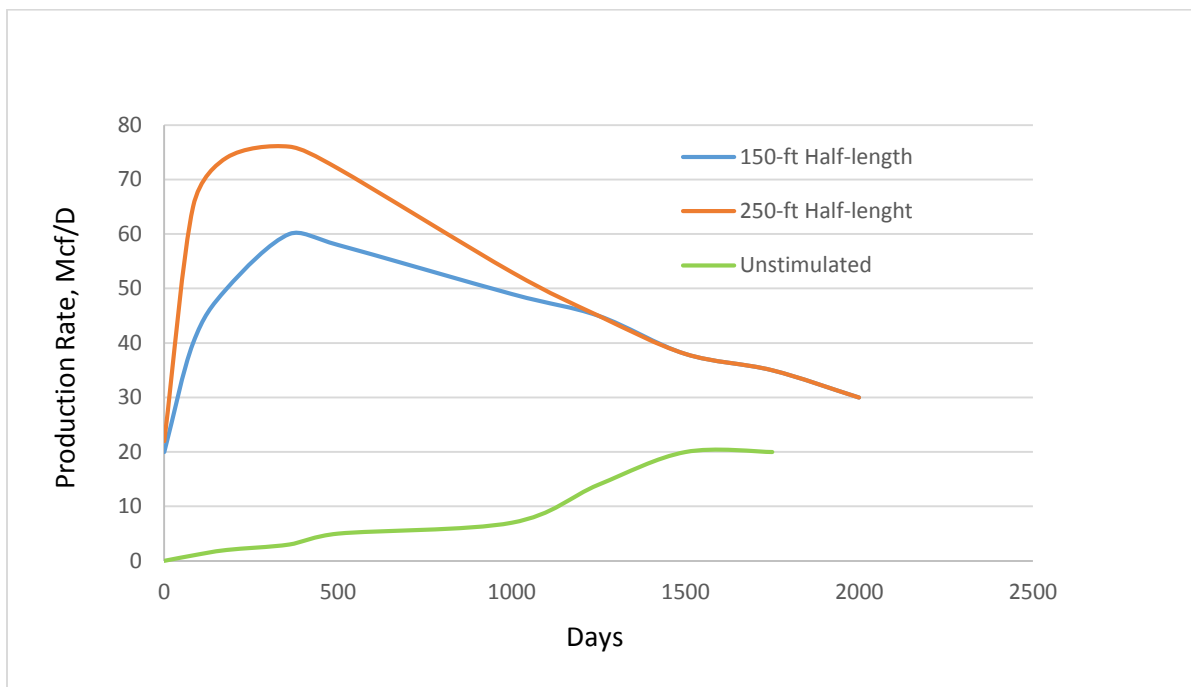


Figure 2.4: Effect of fracture on production rates *Source: (Jikich, McLendon, & Smith).*

As it can be seen from figure 2.4, the production rate can be improved by hydraulic fracture. The blue line profile in the figure shows production before stimulation. As the fracture length is increased, production also increases. This can be seen by looking at the green and red production rate profiles in the graph. As time increases, the fracture length tends not to have an effect on the production rate.

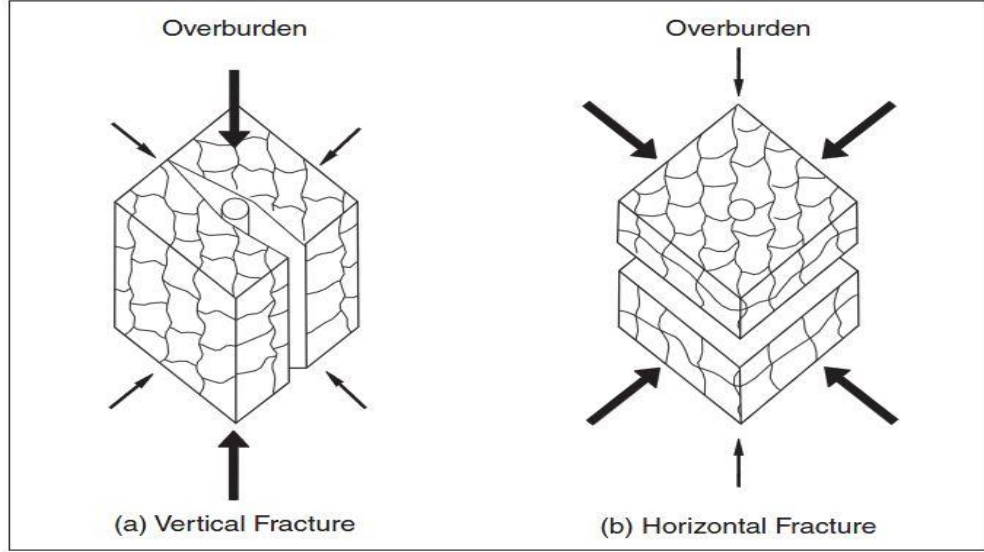


Figure 2.5: Stresses fracture orientation in coals *Source: (Hoyer, 1991).*

### 2.5.1 Fracture Width Modeling

When a coal formation is under stress, a highly non-linear deformation behavior is observed due to the cleat system. A research by (Abass, Kim, & Hedayati, 1991) suggests the use of the following approach, based on elastic deformation, in order to determine the minimum fracture width in coal seams for a given treatment pressure, during hydraulic fracturing process. The deformation of the coal is given by the following equation (Abass et al., 1991):

$$\epsilon = \frac{1}{E} [\sigma_1 - \nu (\sigma_2 + \sigma_3)] \quad (\text{Eq.3})$$

The strain can then be substituted by the following expression:

$$\epsilon = \frac{W}{D} \quad (\text{Eq. 4})$$

Where, **W** is fracture width and **D** is distance through which the effect elastic deformation will be felt in the rock. Combining both equations 4 and 5, the final expression can be obtained:

$$\Delta W = \frac{D}{E} [\Delta P - \nu (\sigma_2 + \sigma_3)] \quad (\text{Eq.5})$$

## 2.5.2 Types of fracturing Fluids for Coal

There are five fluids used to fracture coal formations during hydraulic fracturing process: Water with proppant, water without proppant, linear polymer, crosslinked gel and nitrogen foam. The table below describes the ratings of each type of fracturing fluid with respect to the general cost in the industry.

Table 2.3 Types of fracture fluids used in coal. *Source: (Mavko et al., 1986).*

| <b>Fracturing fluid</b>       | <b>Cost</b> | <b>Formation damage</b> | <b>Proppant placement</b> | <b>Propped length (ft)</b> |
|-------------------------------|-------------|-------------------------|---------------------------|----------------------------|
| <b>Water with proppant</b>    | Good        | Good                    | Poor                      | Poor                       |
| <b>Water without proppant</b> | Good        | Good                    | Poor                      | Poor                       |
| <b>Linear Polymer</b>         | Fair        | Poor                    | Fair                      | Fair                       |
| <b>Crosslinked Gel</b>        | Fair        | Poor                    | High                      | High                       |
| <b>Nitrogen foam</b>          | High        | Good                    | Good                      | Good                       |

Water is cheaper than the polymers, crosslinked gels and nitrogen foam, therefore it is considered to be of good cost. However, water produces lower (poor) fracture length compared to the other types of fracturing fluids. The cost and the fracture length of the linear polymer fluids is considered fair, that is, not too expensive and fairly good fracture length.

## CHAPTER 3: METHODOLOGY

To achieve the objectives of this research few methods will be used. Before all, data gathering is conducted. Data gathering consists of collection of information from various sources, such as journals, previous research papers text books and other relevant types of publication. For optimal analysis and accurate results three data sets will be analyzed from different CBM fields listed below:

- Powder River,
- San Juan Basin,
- Sarawak coalfield.

The next step will be to apply hydraulic fracturing model to generate a set of permeability and porosity variations due to the fracture process. These values will then be used in Eclipse. Eclipse E300 will be used in order to perform the sensitivity analysis of the effect of permeability and porosity variations of coal bed methane fields in order to enhance or optimize CBM production.

The eclipse software is provided in the reservoir simulation laboratories of the university hence it will be of easy access. For this research, eclipse data will be used as well as the data from publications.

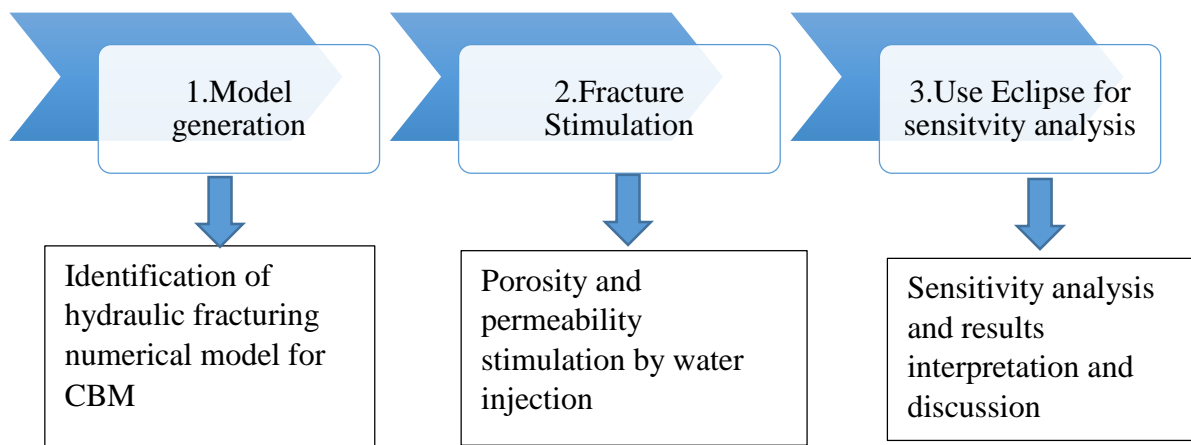


Figure 3.1: Project's methodology steps



### 3.1 General Activities Flowchart

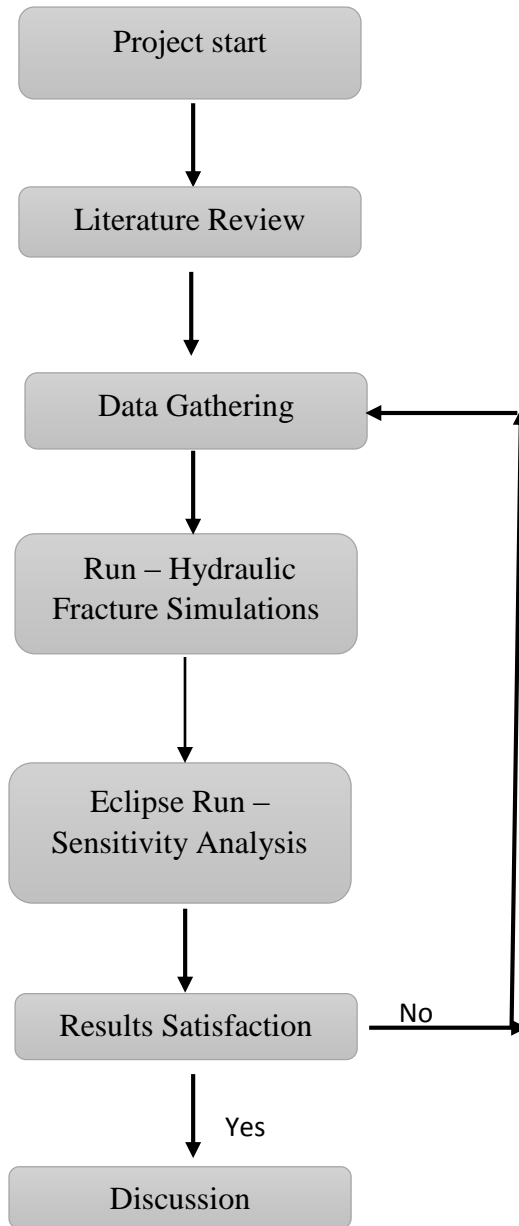


Figure 3.2: General project activities flow

The results satisfaction is based on the sensitivity analysis of the natural gas production rate from each of the case studies. Percentage of increment of the production rates is determined and interpreted to determine to analyze the effect of the stimulation of the CBM formations.

### 3.2 General Project Milestones and Gantt chart

The figure and table below show how project tasks are allocated and duration time of each task throughout the project life time (FYP 1 and FYP 2).

Table 3.1: Project activities and deadlines during FYP 1.

| Detail/Week                     | 1 | 2 | 3 | 4 | 5 | 6 | 7 | 8 | 9 | 10 | 11 | 12 | 13 | 14 |
|---------------------------------|---|---|---|---|---|---|---|---|---|----|----|----|----|----|
| Selection of Project            | ■ | ■ | ■ |   |   |   |   |   |   |    |    |    |    |    |
| Preliminary Research Work       |   |   |   | ■ | ■ | ■ |   |   |   |    |    |    |    |    |
| Submission of Extended Proposal |   |   |   |   |   |   |   | ● |   |    |    |    |    |    |
| Proposal Defense                |   |   |   |   |   |   |   |   | ■ | ■  | ■  | ■  |    |    |
| Project work Continues          |   |   |   |   |   |   |   |   | ■ | ■  | ■  | ■  |    |    |
| Submission of Interim Draft     |   |   |   |   |   |   |   |   |   |    |    |    | ●  |    |
| Submission of Interim Report    |   |   |   |   |   |   |   |   |   |    |    |    |    | ●  |

Deliverables ●  
Progress ■

Table 3.2: project key milestones for FYP 2

| Detail/week                    | 1 | 2 | 3 | 4 | 5 | 6 | 7 | 8 | 9 | 10 | 11 | 12 | 13 | 14 |
|--------------------------------|---|---|---|---|---|---|---|---|---|----|----|----|----|----|
| Project research work/Findings | ■ | ■ | ■ | ■ | ■ | ■ |   |   |   |    |    |    |    |    |
| Lab simulation                 |   |   |   | ■ | ■ | ■ | ■ | ■ | ■ |    |    |    |    |    |
| Progress report                |   |   |   |   |   |   | ● |   |   |    |    |    |    |    |
| Project work continues         |   |   |   |   |   |   |   | ■ | ■ | ■  | ■  | ■  |    |    |
| Pre- sedex/poster exhibition   |   |   |   |   |   |   |   |   | ● |    |    |    |    |    |
| Final draft report submission  |   |   |   |   |   |   |   |   |   |    |    | ●  |    |    |
| Final oral presentation/Viva   |   |   |   |   |   |   |   |   |   |    |    |    |    | ●  |

## CHAPTER 4: RESULTS AND DISCUSSION

### 4.1 Coal Flow Mechanism Analysis

Coals seams can be described as heterogeneous porous medium with low permeability channels and pore spaces. The fluid flow mechanisms in coal occurs in two step process: the first step is characterized by the fast gas diffusion from the micropores of the coal matrix into the larger cracks due to the presence of micro cracks. Second step gas flows laminarly through the cracks into the wellbore. The first process is described by Fick's law of diffusion whereas the second flow is described by Darcy's law.

$$q = -DA \frac{dC}{dL} \quad \text{Fick's Law} \quad (\text{Eq. 4.1})$$

$$q = -\frac{KA}{\mu} \frac{dP}{dL} \quad \text{Darcy's Law} \quad (\text{Eq.4.2})$$

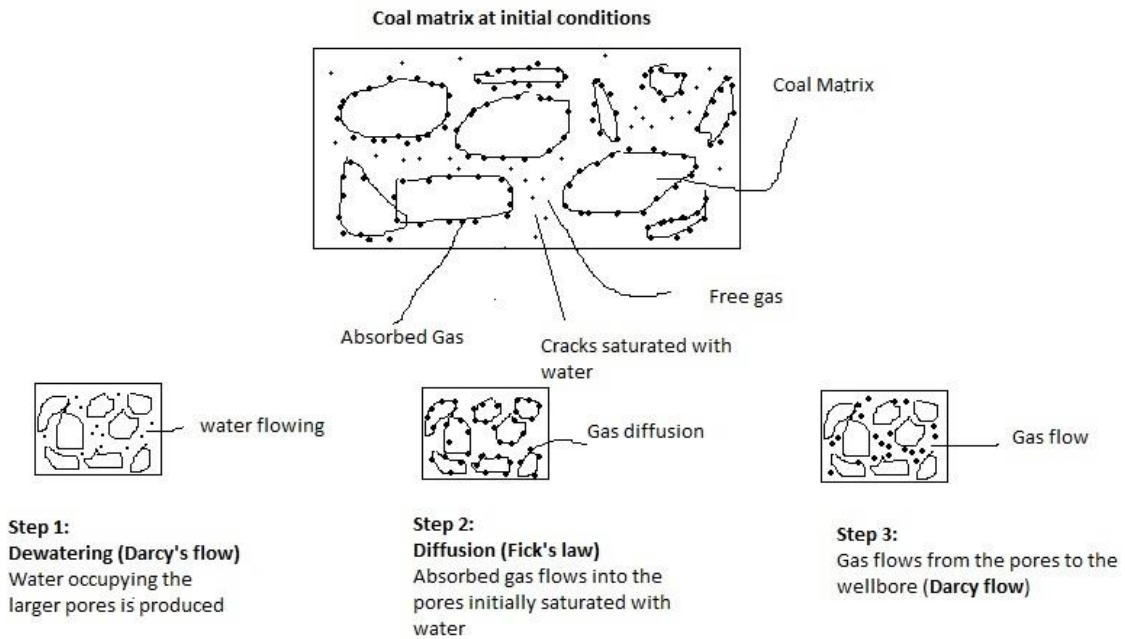


Figure 4.1.1: schematic analysis of flow mechanisms in coal

In the figure above it can be clearly observed that the governing fluid flow regime in production of methane from coal is Darcy flow. The diffusion process happens as a subsequent flow caused by the Darcy dewatering process.

## 4.2 Hydraulic Fracturing Stimulation Results

Keshavarz et al. (2014) developed a model for stimulation of coal bed reservoirs by hydraulic fracturing. This mathematical model will be used in this research to simulate the changes in permeability and porosity of coal.

$$K(r) = K_0 \left[ 1 - \frac{q\mu C_f (1+\nu)}{2\pi K_0 (1+\nu)} \ln \frac{r}{r_e} \right] \quad (\text{Eq.4.2.1})$$

Porosity variations are given by the following relationship:

$$\frac{k}{K_0} = \left( \frac{\phi}{\phi_0} \right)^3 \quad (\text{Eq. 4.2.2})$$

These mathematical relationships were developed based on the following assumptions (Keshavarz et al., 2014):

1. Isotropic horizontal stress and permeability and fluid flow is described by Darcy's law.
2. Elastic formation during both injection and production, and no failure occurs.
3. Reservoir under plain strain condition.
4. Only natural fractures are stimulated ( $P_{inj} < P_b$ ).
5. The injection fluid is incompressible.
6. Steady- state and vertical flow neglected.
7. The shrinkage of coal due to gas desorption is neglected.

## Permeability and porosity Stimulation

Appendix B shows base case reservoir properties data table of three coal basins. Powder River and San Juan basin are located in the US and Sarawak field located in Malaysia. By assuming water injection, permeability and porosity changes are simulated and results are recorded. The simulation process concentrates on the analysis of permeability and porosity changes caused by water injection at various injection flow rates.

### Case 1: Powder River Basin

#### Input Parameters

|                                      |        |  |   |
|--------------------------------------|--------|--|---|
| <b>Type of Injection Fluid:</b>      | Water  | <b>Drainage radius (re):</b>                   | 350 ft                                  |
| <b>Viscosity (<math>\mu</math>):</b> | 1.0 cp | <b>Initial permeability (k<sub>o</sub>):</b>   | 300md                                   |
| <b>Coal passion's ratio:</b>         | 0.3    | <b>Initial Porosity (<math>\phi_0</math>):</b> | 0.02                                    |
| <b>Wellbore radius(r):</b>           | 0.32ft | <b>Coal compressibility (cf):</b>              | $1.0 \times 10^{-6}$ psia <sup>-1</sup> |

| PHIO | k0  | qinj | u | cf       | v   | r    | re  | pi   | n        | d      | ln       | Kinj     | K/K0     | FI   |
|------|-----|------|---|----------|-----|------|-----|------|----------|--------|----------|----------|----------|------|
| 0.02 | 300 | 50   | 1 | 0.000001 | 0.3 | 0.32 | 350 | 3.14 | 0.000065 | 1318.8 | -6.99737 | 300.0001 | 1        | 0.02 |
| 0.02 | 300 | 75   | 1 | 0.000001 | 0.3 | 0.32 | 350 | 3.14 | 9.75E-05 | 1318.8 | -6.99737 | 300.0002 | 1.000001 | 0.02 |
| 0.02 | 300 | 100  | 1 | 0.000001 | 0.3 | 0.32 | 350 | 3.14 | 0.00013  | 1318.8 | -6.99737 | 300.0002 | 1.000001 | 0.02 |
| 0.02 | 300 | 125  | 1 | 0.000001 | 0.3 | 0.32 | 350 | 3.14 | 0.000163 | 1318.8 | -6.99737 | 300.0003 | 1.000001 | 0.02 |
| 0.02 | 300 | 150  | 1 | 0.000001 | 0.3 | 0.32 | 350 | 3.14 | 0.000195 | 1318.8 | -6.99737 | 300.0003 | 1.000001 | 0.02 |
| 0.02 | 300 | 175  | 1 | 0.000001 | 0.3 | 0.32 | 350 | 3.14 | 0.000228 | 1318.8 | -6.99737 | 300.0004 | 1.000001 | 0.02 |
| 0.02 | 300 | 200  | 1 | 0.000001 | 0.3 | 0.32 | 350 | 3.14 | 0.00026  | 1318.8 | -6.99737 | 300.0004 | 1.000001 | 0.02 |
| 0.02 | 300 | 225  | 1 | 0.000001 | 0.3 | 0.32 | 350 | 3.14 | 0.000293 | 1318.8 | -6.99737 | 300.0005 | 1.000002 | 0.02 |
| 0.02 | 300 | 250  | 1 | 0.000001 | 0.3 | 0.32 | 350 | 3.14 | 0.000325 | 1318.8 | -6.99737 | 300.0005 | 1.000002 | 0.02 |
| 0.02 | 300 | 275  | 1 | 0.000001 | 0.3 | 0.32 | 350 | 3.14 | 0.000358 | 1318.8 | -6.99737 | 300.0006 | 1.000002 | 0.02 |
| 0.02 | 300 | 300  | 1 | 0.000001 | 0.3 | 0.32 | 350 | 3.14 | 0.00039  | 1318.8 | -6.99737 | 300.0006 | 1.000002 | 0.02 |
| 0.02 | 300 | 325  | 1 | 0.000001 | 0.3 | 0.32 | 350 | 3.14 | 0.000423 | 1318.8 | -6.99737 | 300.0007 | 1.000002 | 0.02 |
| 0.02 | 300 | 350  | 1 | 0.000001 | 0.3 | 0.32 | 350 | 3.14 | 0.000455 | 1318.8 | -6.99737 | 300.0007 | 1.000002 | 0.02 |
| 0.02 | 300 | 400  | 1 | 0.000001 | 0.3 | 0.32 | 350 | 3.14 | 0.00052  | 1318.8 | -6.99737 | 300.0008 | 1.000003 | 0.02 |
| 0.02 | 300 | 450  | 1 | 0.000001 | 0.3 | 0.32 | 350 | 3.14 | 0.000585 | 1318.8 | -6.99737 | 300.0009 | 1.000003 | 0.02 |
| 0.02 | 300 | 500  | 1 | 0.000001 | 0.3 | 0.32 | 350 | 3.14 | 0.00065  | 1318.8 | -6.99737 | 300.001  | 1.000003 | 0.02 |
| 0.02 | 300 | 550  | 1 | 0.000001 | 0.3 | 0.32 | 350 | 3.14 | 0.000715 | 1318.8 | -6.99737 | 300.0011 | 1.000004 | 0.02 |
| 0.02 | 300 | 600  | 1 | 0.000001 | 0.3 | 0.32 | 350 | 3.14 | 0.00078  | 1318.8 | -6.99737 | 300.0012 | 1.000004 | 0.02 |
| 0.02 | 300 | 650  | 1 | 0.000001 | 0.3 | 0.32 | 350 | 3.14 | 0.000845 | 1318.8 | -6.99737 | 300.0013 | 1.000004 | 0.02 |
| 0.02 | 300 | 700  | 1 | 0.000001 | 0.3 | 0.32 | 350 | 3.14 | 0.00091  | 1318.8 | -6.99737 | 300.0014 | 1.000005 | 0.02 |
| 0.02 | 300 | 750  | 1 | 0.000001 | 0.3 | 0.32 | 350 | 3.14 | 0.000975 | 1318.8 | -6.99737 | 300.0016 | 1.000005 | 0.02 |
| 0.02 | 300 | 800  | 1 | 0.000001 | 0.3 | 0.32 | 350 | 3.14 | 0.00104  | 1318.8 | -6.99737 | 300.0017 | 1.000006 | 0.02 |
| 0.02 | 300 | 850  | 1 | 0.000001 | 0.3 | 0.32 | 350 | 3.14 | 0.001105 | 1318.8 | -6.99737 | 300.0018 | 1.000006 | 0.02 |
| 0.02 | 300 | 950  | 1 | 0.000001 | 0.3 | 0.32 | 350 | 3.14 | 0.001235 | 1318.8 | -6.99737 | 300.002  | 1.000007 | 0.02 |
| 0.02 | 300 | 1050 | 1 | 0.000001 | 0.3 | 0.32 | 350 | 3.14 | 0.001365 | 1318.8 | -6.99737 | 300.0022 | 1.000007 | 0.02 |
| 0.02 | 300 | 1200 | 1 | 0.000001 | 0.3 | 0.32 | 350 | 3.14 | 0.00156  | 1318.8 | -6.99737 | 300.0025 | 1.000008 | 0.02 |

Figure 4.2.1: Determination of the injection permeability for the Powder River reservoir

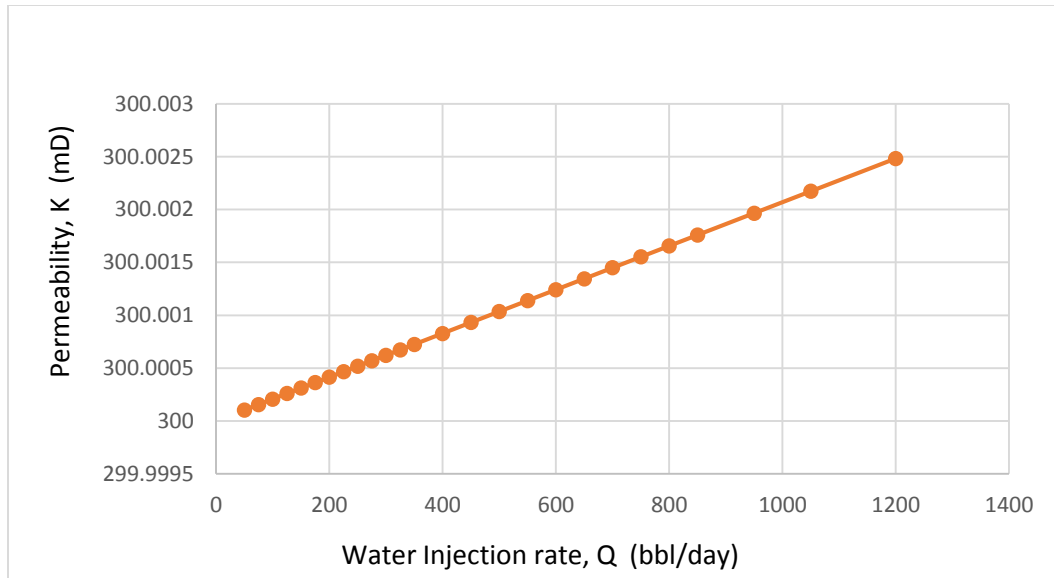


Figure 4.2.2: Fluid injection rate vs permeability change for Powder River reservoir

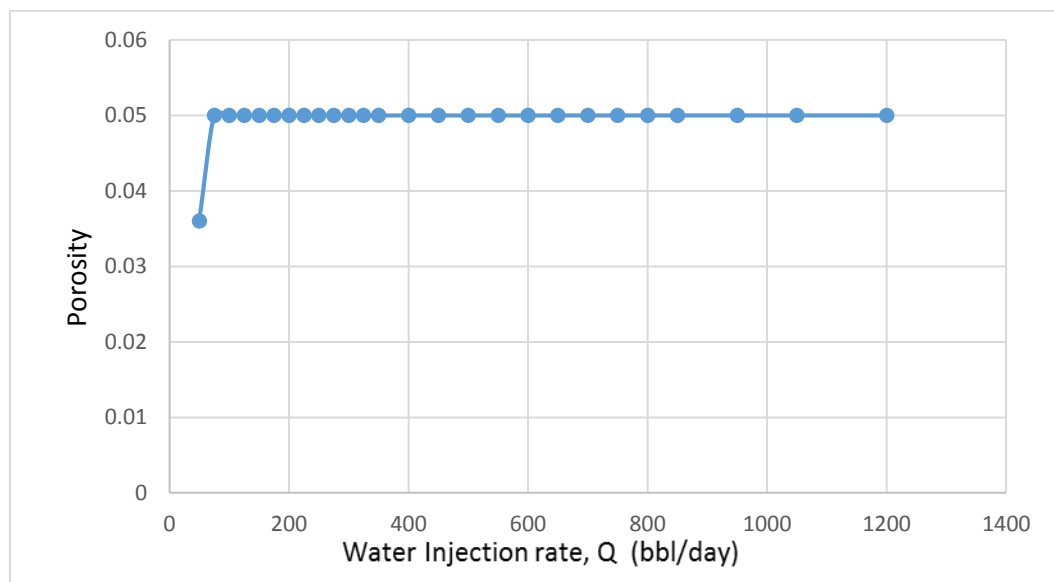


Figure 4.2.3: Fluid injection rate vs porosity change for Powder River reservoir

From the graphs above it can be observed that hydraulic fracture can improve the permeability and the porosity of coal. As the fluid injection rate is increased, the permeability of the coal increases as well.

## Case 2: San Juan Basin

### Input Parameters

|                                      |        |  |   |
|--------------------------------------|--------|--|---|
| <b>Type of Injection Fluid:</b>      | Water  | <b>Drainage radius (re):</b>                   | 400 ft                                  |
| <b>Viscosity (<math>\mu</math>):</b> | 1.0 cp | <b>Initial permeability (k<sub>o</sub>):</b>   | 3.65md                                  |
| <b>Coal passion's ratio:</b>         | 0.3    | <b>Initial Porosity (<math>\phi_0</math>):</b> | 0.05                                    |
| <b>Wellbore radius(r):</b>           | 0.30ft | <b>Coal compressibility (cf):</b>              | $1.0 \times 10^{-6}$ psia <sup>-1</sup> |

| PHIO | k0   | qinj | u | cf       | v   | r   | re  | pi   | n        | d       | ln       | Kinj     | K/K0     | FI        |
|------|------|------|---|----------|-----|-----|-----|------|----------|---------|----------|----------|----------|-----------|
| 0.05 | 3.65 | 50   | 1 | 0.000001 | 0.3 | 0.3 | 400 | 3.14 | 0.000065 | 16.0454 | -7.19544 | 3.650106 | 1.000029 | 0.05      |
| 0.05 | 3.65 | 75   | 1 | 0.000001 | 0.3 | 0.3 | 400 | 3.14 | 9.75E-05 | 16.0454 | -7.19544 | 3.65016  | 1.000044 | 0.0500001 |
| 0.05 | 3.65 | 100  | 1 | 0.000001 | 0.3 | 0.3 | 400 | 3.14 | 0.00013  | 16.0454 | -7.19544 | 3.650213 | 1.000058 | 0.0500001 |
| 0.05 | 3.65 | 125  | 1 | 0.000001 | 0.3 | 0.3 | 400 | 3.14 | 0.000163 | 16.0454 | -7.19544 | 3.650266 | 1.000073 | 0.0500001 |
| 0.05 | 3.65 | 150  | 1 | 0.000001 | 0.3 | 0.3 | 400 | 3.14 | 0.000195 | 16.0454 | -7.19544 | 3.650319 | 1.000087 | 0.0500001 |
| 0.05 | 3.65 | 175  | 1 | 0.000001 | 0.3 | 0.3 | 400 | 3.14 | 0.000228 | 16.0454 | -7.19544 | 3.650372 | 1.000102 | 0.0500002 |
| 0.05 | 3.65 | 200  | 1 | 0.000001 | 0.3 | 0.3 | 400 | 3.14 | 0.00026  | 16.0454 | -7.19544 | 3.650426 | 1.000117 | 0.0500002 |
| 0.05 | 3.65 | 225  | 1 | 0.000001 | 0.3 | 0.3 | 400 | 3.14 | 0.000293 | 16.0454 | -7.19544 | 3.650479 | 1.000131 | 0.0500002 |
| 0.05 | 3.65 | 250  | 1 | 0.000001 | 0.3 | 0.3 | 400 | 3.14 | 0.000325 | 16.0454 | -7.19544 | 3.650532 | 1.000146 | 0.0500002 |
| 0.05 | 3.65 | 275  | 1 | 0.000001 | 0.3 | 0.3 | 400 | 3.14 | 0.000358 | 16.0454 | -7.19544 | 3.650585 | 1.00016  | 0.0500003 |
| 0.05 | 3.65 | 300  | 1 | 0.000001 | 0.3 | 0.3 | 400 | 3.14 | 0.00039  | 16.0454 | -7.19544 | 3.650638 | 1.000175 | 0.0500003 |
| 0.05 | 3.65 | 325  | 1 | 0.000001 | 0.3 | 0.3 | 400 | 3.14 | 0.000423 | 16.0454 | -7.19544 | 3.650692 | 1.000189 | 0.0500003 |
| 0.05 | 3.65 | 350  | 1 | 0.000001 | 0.3 | 0.3 | 400 | 3.14 | 0.000455 | 16.0454 | -7.19544 | 3.650745 | 1.000204 | 0.0500003 |
| 0.05 | 3.65 | 400  | 1 | 0.000001 | 0.3 | 0.3 | 400 | 3.14 | 0.00052  | 16.0454 | -7.19544 | 3.650851 | 1.000233 | 0.0500004 |
| 0.05 | 3.65 | 450  | 1 | 0.000001 | 0.3 | 0.3 | 400 | 3.14 | 0.000585 | 16.0454 | -7.19544 | 3.650958 | 1.000262 | 0.0500004 |
| 0.05 | 3.65 | 500  | 1 | 0.000001 | 0.3 | 0.3 | 400 | 3.14 | 0.00065  | 16.0454 | -7.19544 | 3.651064 | 1.000291 | 0.0500005 |
| 0.05 | 3.65 | 550  | 1 | 0.000001 | 0.3 | 0.3 | 400 | 3.14 | 0.000715 | 16.0454 | -7.19544 | 3.65117  | 1.000321 | 0.0500005 |
| 0.05 | 3.65 | 600  | 1 | 0.000001 | 0.3 | 0.3 | 400 | 3.14 | 0.00078  | 16.0454 | -7.19544 | 3.651277 | 1.00035  | 0.0500006 |
| 0.05 | 3.65 | 650  | 1 | 0.000001 | 0.3 | 0.3 | 400 | 3.14 | 0.000845 | 16.0454 | -7.19544 | 3.651383 | 1.000379 | 0.0500006 |
| 0.05 | 3.65 | 700  | 1 | 0.000001 | 0.3 | 0.3 | 400 | 3.14 | 0.00091  | 16.0454 | -7.19544 | 3.65149  | 1.000408 | 0.0500007 |
| 0.05 | 3.65 | 750  | 1 | 0.000001 | 0.3 | 0.3 | 400 | 3.14 | 0.000975 | 16.0454 | -7.19544 | 3.651596 | 1.000437 | 0.0500007 |
| 0.05 | 3.65 | 800  | 1 | 0.000001 | 0.3 | 0.3 | 400 | 3.14 | 0.00104  | 16.0454 | -7.19544 | 3.651702 | 1.000466 | 0.0500008 |
| 0.05 | 3.65 | 850  | 1 | 0.000001 | 0.3 | 0.3 | 400 | 3.14 | 0.001105 | 16.0454 | -7.19544 | 3.651809 | 1.000496 | 0.0500008 |
| 0.05 | 3.65 | 950  | 1 | 0.000001 | 0.3 | 0.3 | 400 | 3.14 | 0.001235 | 16.0454 | -7.19544 | 3.652021 | 1.000554 | 0.0500009 |
| 0.05 | 3.65 | 1050 | 1 | 0.000001 | 0.3 | 0.3 | 400 | 3.14 | 0.001365 | 16.0454 | -7.19544 | 3.652234 | 1.000612 | 0.050001  |
| 0.05 | 3.65 | 1200 | 1 | 0.000001 | 0.3 | 0.3 | 400 | 3.14 | 0.00156  | 16.0454 | -7.19544 | 3.652553 | 1.0007   | 0.0500012 |

Figure 4.2.4: Determination of the injection permeability for the San Juan basin

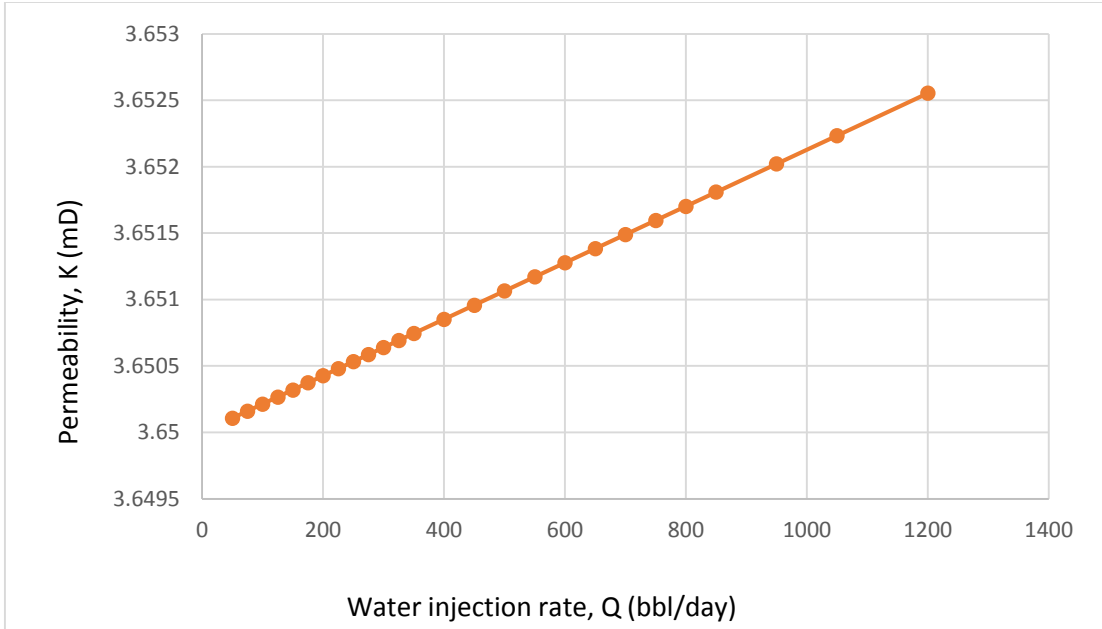


Figure 4.2.5: Fluid injection rate vs permeability change for San Juan reservoir

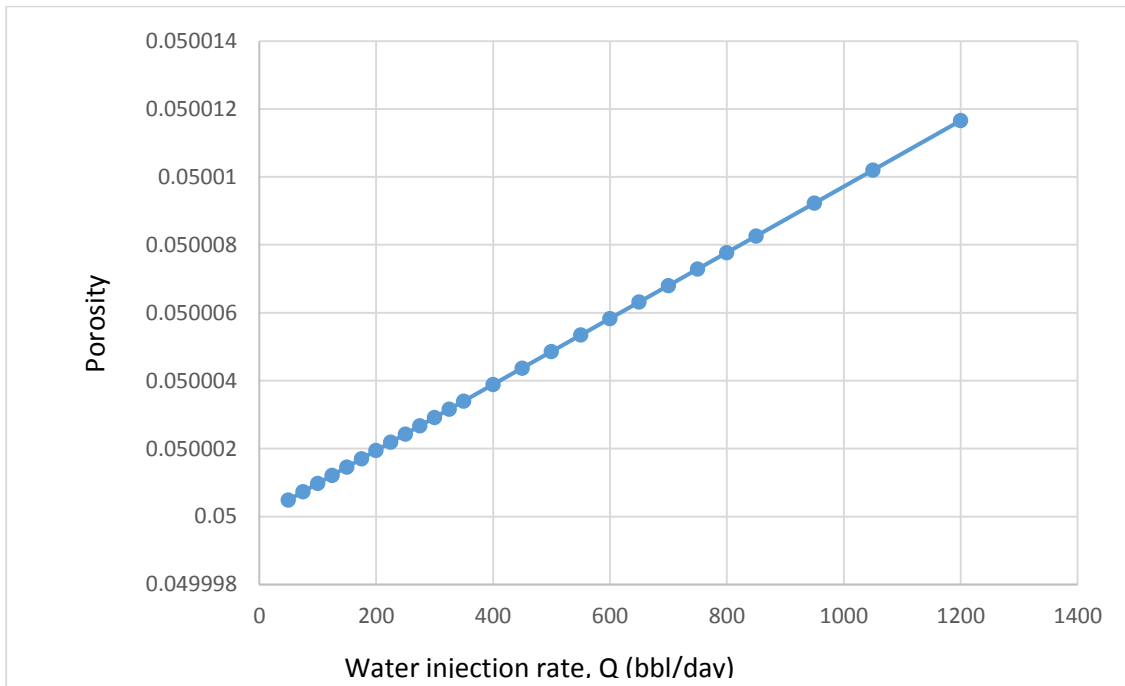


Figure 4.2.6: Fluid injection rate vs permeability change for San Juan reservoir



### Case 3: Sarawak Coalfield

#### Input Parameters

|                                      |        |  |   |
|--------------------------------------|--------|--|---|
| <b>Type of Injection Fluid:</b>      | Water  | <b>Drainage radius (re):</b>                   | 250 ft                                  |
| <b>Viscosity (<math>\mu</math>):</b> | 1.0 cp | <b>Initial permeability (k<sub>o</sub>):</b>   | 14.42md                                 |
| <b>Coal passion's ratio:</b>         | 0.3    | <b>Initial Porosity (<math>\phi_0</math>):</b> | 0.036                                   |
| <b>Wellbore radius(r):</b>           | 0.28ft | <b>Coal compressibility (cf):</b>              | $1.0 \times 10^{-6}$ psia <sup>-1</sup> |

| PHIO  | k0    | qinj | u | cf       | v   | r    | re  | pi   | n        | d        | ln       | Kinj     | K/K0     | FI       |
|-------|-------|------|---|----------|-----|------|-----|------|----------|----------|----------|----------|----------|----------|
| 0.036 | 14.42 | 50   | 1 | 0.000001 | 0.3 | 0.28 | 250 | 3.14 | 0.000065 | 63.39032 | -6.79443 | 14.4201  | 1.000007 | 0.036    |
| 0.05  | 14.42 | 75   | 1 | 0.000001 | 0.3 | 0.28 | 250 | 3.14 | 9.75E-05 | 63.39032 | -6.79443 | 14.42015 | 1.000001 | 0.05     |
| 0.05  | 14.42 | 100  | 1 | 0.000001 | 0.3 | 0.28 | 250 | 3.14 | 0.00013  | 63.39032 | -6.79443 | 14.4202  | 1.000014 | 0.05     |
| 0.05  | 14.42 | 125  | 1 | 0.000001 | 0.3 | 0.28 | 250 | 3.14 | 0.000163 | 63.39032 | -6.79443 | 14.42025 | 1.000017 | 0.05     |
| 0.05  | 14.42 | 150  | 1 | 0.000001 | 0.3 | 0.28 | 250 | 3.14 | 0.000195 | 63.39032 | -6.79443 | 14.4203  | 1.000021 | 0.05     |
| 0.05  | 14.42 | 175  | 1 | 0.000001 | 0.3 | 0.28 | 250 | 3.14 | 0.000228 | 63.39032 | -6.79443 | 14.42035 | 1.000024 | 0.05     |
| 0.05  | 14.42 | 200  | 1 | 0.000001 | 0.3 | 0.28 | 250 | 3.14 | 0.00026  | 63.39032 | -6.79443 | 14.4204  | 1.000028 | 0.05     |
| 0.05  | 14.42 | 225  | 1 | 0.000001 | 0.3 | 0.28 | 250 | 3.14 | 0.000293 | 63.39032 | -6.79443 | 14.42045 | 1.000031 | 0.050001 |
| 0.05  | 14.42 | 250  | 1 | 0.000001 | 0.3 | 0.28 | 250 | 3.14 | 0.000325 | 63.39032 | -6.79443 | 14.4205  | 1.000035 | 0.050001 |
| 0.05  | 14.42 | 275  | 1 | 0.000001 | 0.3 | 0.28 | 250 | 3.14 | 0.000358 | 63.39032 | -6.79443 | 14.42055 | 1.000038 | 0.050001 |
| 0.05  | 14.42 | 300  | 1 | 0.000001 | 0.3 | 0.28 | 250 | 3.14 | 0.00039  | 63.39032 | -6.79443 | 14.4206  | 1.000042 | 0.050001 |
| 0.05  | 14.42 | 325  | 1 | 0.000001 | 0.3 | 0.28 | 250 | 3.14 | 0.000423 | 63.39032 | -6.79443 | 14.42065 | 1.000045 | 0.050001 |
| 0.05  | 14.42 | 350  | 1 | 0.000001 | 0.3 | 0.28 | 250 | 3.14 | 0.000455 | 63.39032 | -6.79443 | 14.4207  | 1.000049 | 0.050001 |
| 0.05  | 14.42 | 400  | 1 | 0.000001 | 0.3 | 0.28 | 250 | 3.14 | 0.00052  | 63.39032 | -6.79443 | 14.4208  | 1.000056 | 0.050001 |
| 0.05  | 14.42 | 450  | 1 | 0.000001 | 0.3 | 0.28 | 250 | 3.14 | 0.000585 | 63.39032 | -6.79443 | 14.4209  | 1.000063 | 0.050001 |
| 0.05  | 14.42 | 500  | 1 | 0.000001 | 0.3 | 0.28 | 250 | 3.14 | 0.00065  | 63.39032 | -6.79443 | 14.421   | 1.00007  | 0.050001 |
| 0.05  | 14.42 | 550  | 1 | 0.000001 | 0.3 | 0.28 | 250 | 3.14 | 0.000715 | 63.39032 | -6.79443 | 14.42111 | 1.000077 | 0.050001 |
| 0.05  | 14.42 | 600  | 1 | 0.000001 | 0.3 | 0.28 | 250 | 3.14 | 0.00078  | 63.39032 | -6.79443 | 14.42121 | 1.000084 | 0.050001 |
| 0.05  | 14.42 | 650  | 1 | 0.000001 | 0.3 | 0.28 | 250 | 3.14 | 0.000845 | 63.39032 | -6.79443 | 14.42131 | 1.000091 | 0.050002 |
| 0.05  | 14.42 | 700  | 1 | 0.000001 | 0.3 | 0.28 | 250 | 3.14 | 0.00091  | 63.39032 | -6.79443 | 14.42141 | 1.000098 | 0.050002 |
| 0.05  | 14.42 | 750  | 1 | 0.000001 | 0.3 | 0.28 | 250 | 3.14 | 0.000975 | 63.39032 | -6.79443 | 14.42151 | 1.000105 | 0.050002 |
| 0.05  | 14.42 | 800  | 1 | 0.000001 | 0.3 | 0.28 | 250 | 3.14 | 0.00104  | 63.39032 | -6.79443 | 14.42161 | 1.000111 | 0.050002 |
| 0.05  | 14.42 | 850  | 1 | 0.000001 | 0.3 | 0.28 | 250 | 3.14 | 0.001105 | 63.39032 | -6.79443 | 14.42171 | 1.000118 | 0.050002 |
| 0.05  | 14.42 | 950  | 1 | 0.000001 | 0.3 | 0.28 | 250 | 3.14 | 0.001235 | 63.39032 | -6.79443 | 14.42191 | 1.000132 | 0.050002 |
| 0.05  | 14.42 | 1050 | 1 | 0.000001 | 0.3 | 0.28 | 250 | 3.14 | 0.001365 | 63.39032 | -6.79443 | 14.42211 | 1.000146 | 0.050002 |
| 0.05  | 14.42 | 1200 | 1 | 0.000001 | 0.3 | 0.28 | 250 | 3.14 | 0.00156  | 63.39032 | -6.79443 | 14.42241 | 1.000167 | 0.050003 |

Figure 4.2.7: Determination of the injection permeability for the Sarawak reservoir

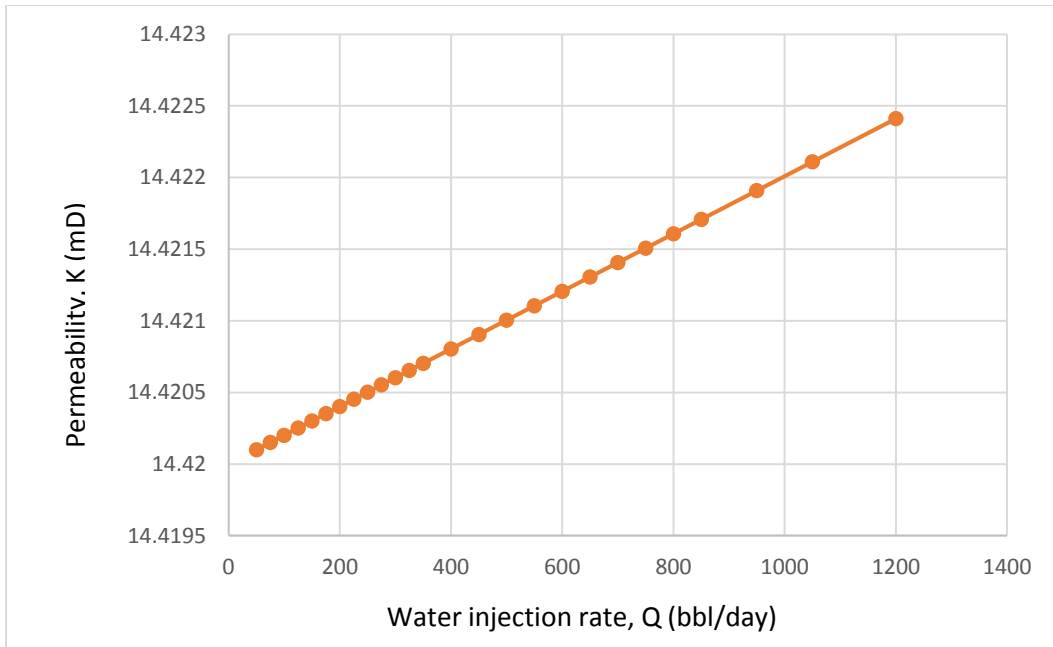


Figure 4.2.8: Fluid injection rate vs permeability change for Sarawak reservoir

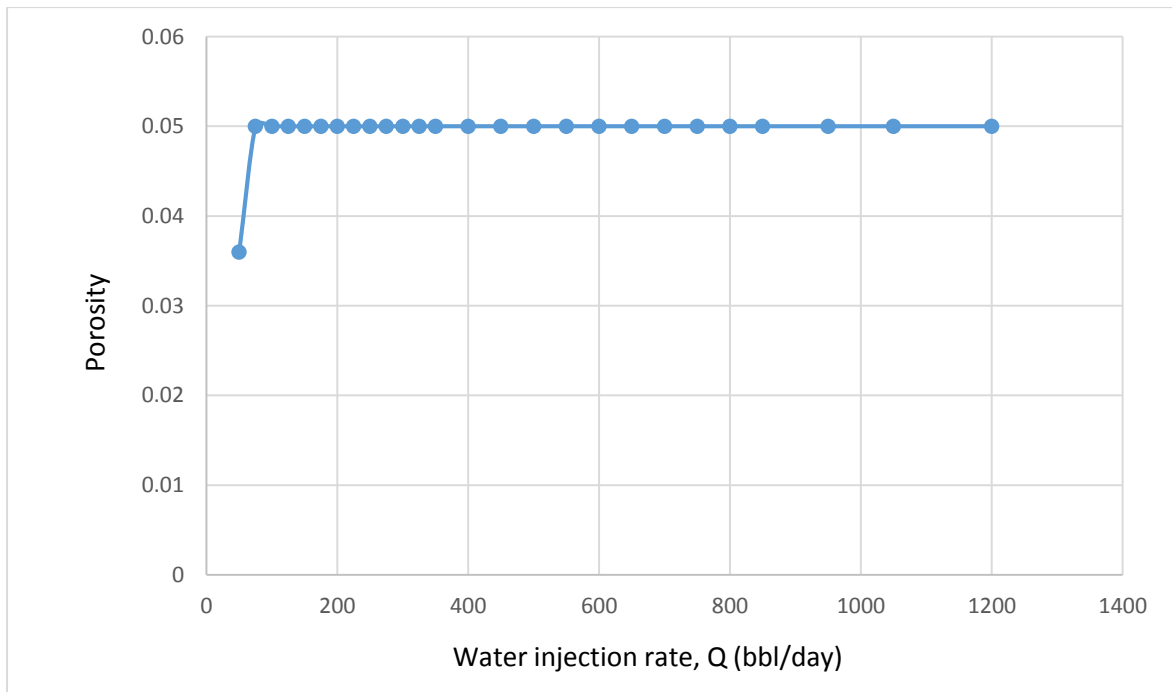


Figure 4.2.9: Fluid injection rate vs permeability change for Sarawak reservoir

As it can be observed from the graphs in all the three case studies, fluid injection in coal bed methane reservoirs can improve the cleat system and hence the productivity. In the Powder River reservoir we can see that permeability changes with fluid injection rate in a straight line. The porosity also increases as result of the increase in the injection rate. In this case however, porosity values change rapidly with increase of injection flow until reaching a point where it becomes constant. Same scenario is observed in the Sarawak reservoir for porosity and permeability variations. In the San Juan reservoir however, the initial permeability and porosity changes are directly proportional to the fluid injection rate. It is also important outline that the amount by which porosity and permeability increased during this simulation is by a small portion that is by 0.01 factors. This can be due to the assumptions made for the mathematical model in use to generate this results only causes small changes. The tendency for porosity to become is related also to the fracture propagation length during the hydraulic fracturing stimulation job.

### 4.3 Eclipse Simulation Results

#### Case 1: Powder River Basin

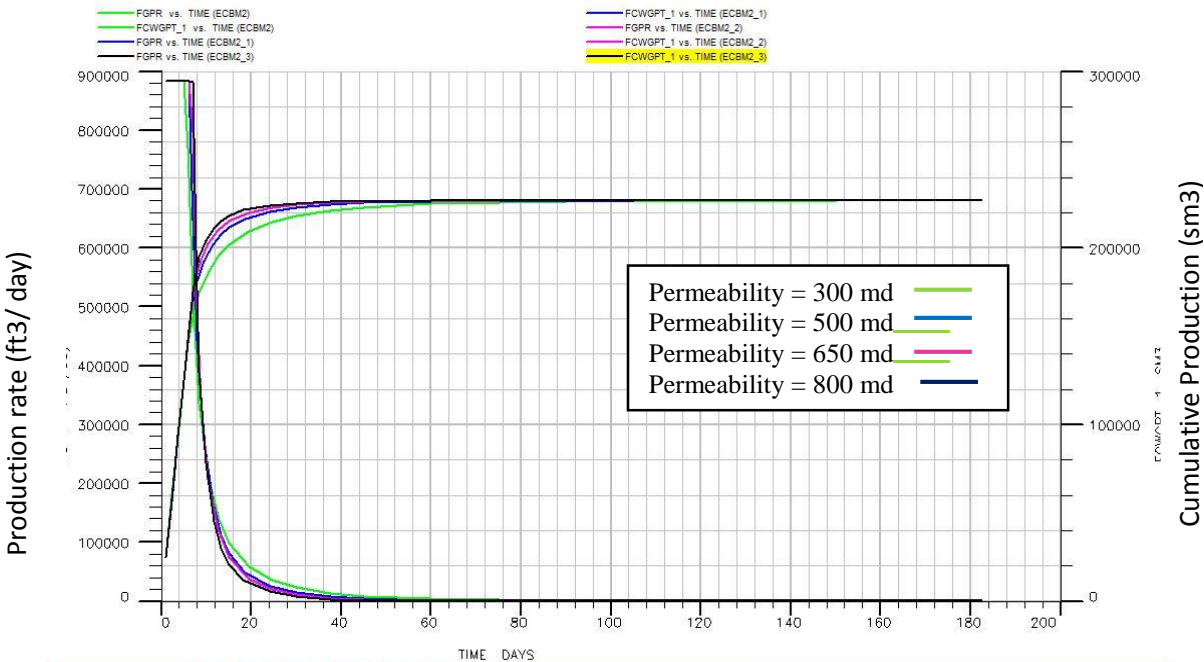


Figure 4.3.1 Field gas production due to variations of permeability vs time (Powder River)

Figure 4.3.1 shows the field gas production rate and the cumulative gas production against production days. The initial permeability of the Powder River basin is 300md. From the graphs it can be seen that as the permeability is increased, the field gas production rate also increases for the first 30 days of production, and decreases to a constant rate as production is continues, until reaching the reservoir total depletion point. Moreover the cumulative gas production increases as permeability increases in the first 40 days, however, as production time continues, the cumulative gas production becomes constant for different values of permeability due to the depletion of the reservoir.

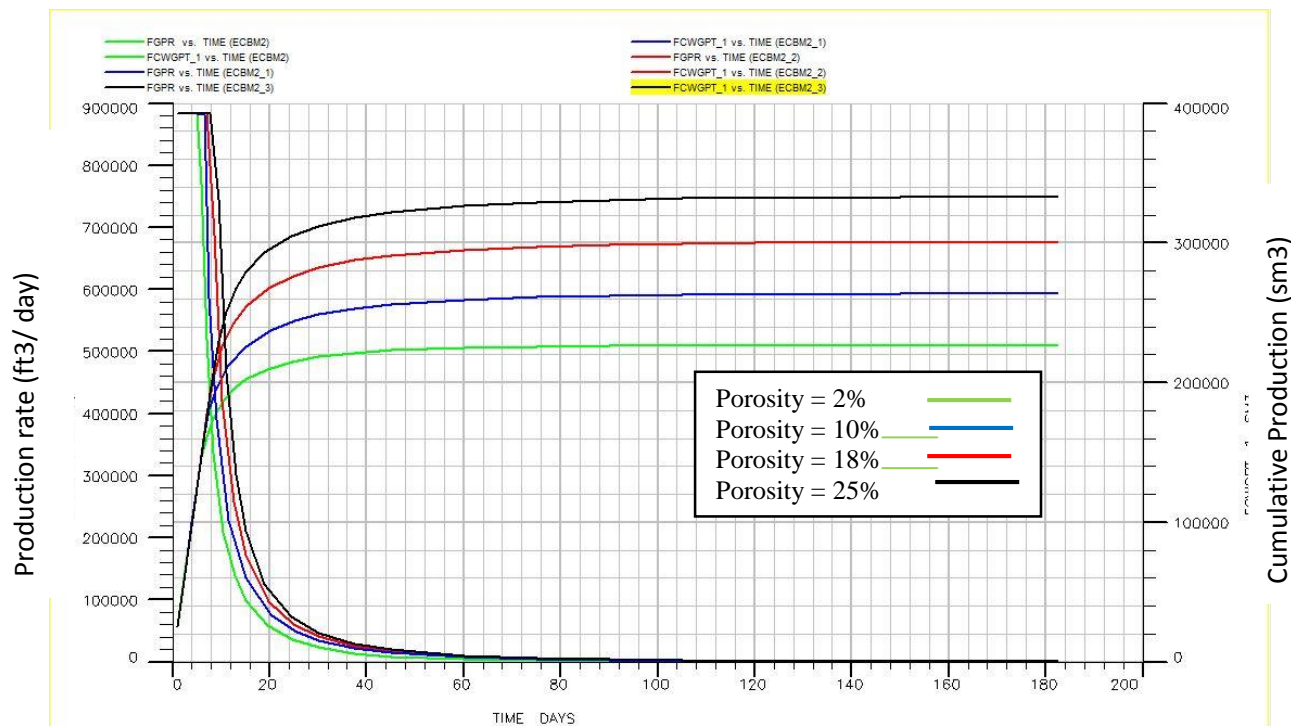


Figure 4.3.2 Field gas production due to porosity changes vs time (Powder River)

In the figure above, it can be seen that as the porosity values are increased from the base case value, the gas production rate increases as well for the first 80 days of production. As production continues, the coal reservoir tends to become constant until reaching total depletion. The same scenario is observed with the cumulative gas production.

**Case 2: San Juan Basin**

**Field gas production due to permeability variations:**

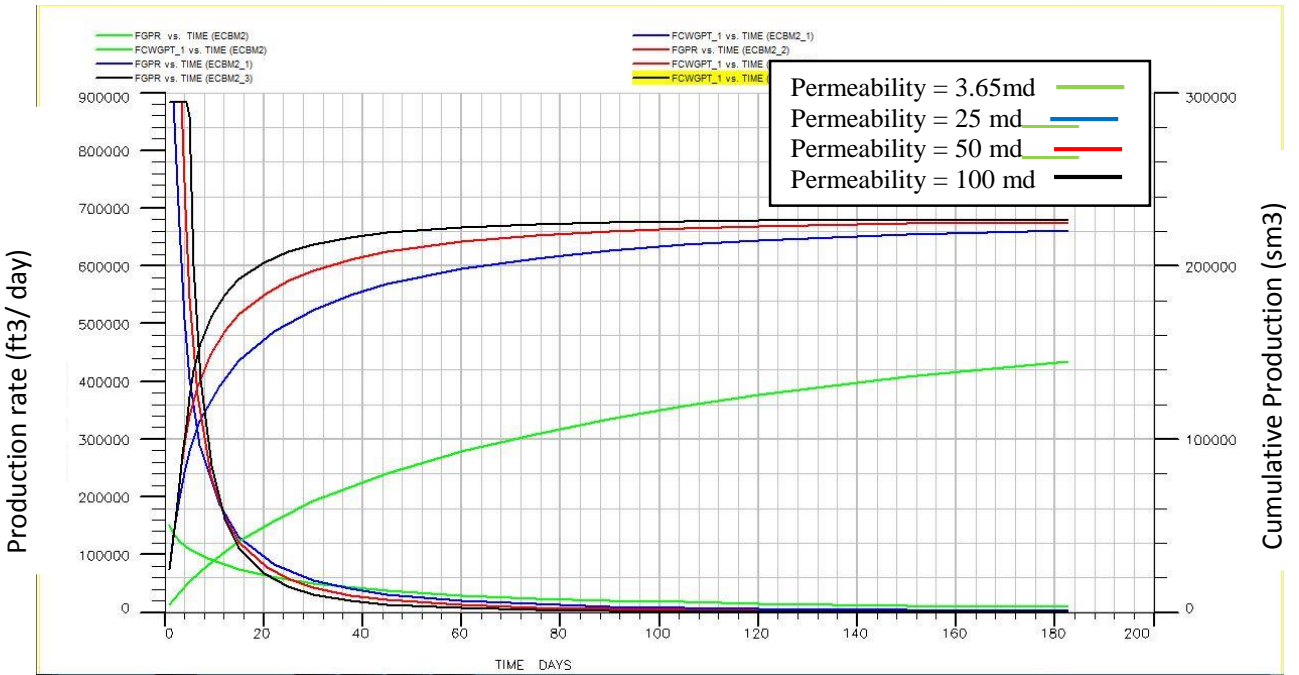


Figure 4.3.3 Field gas production due to permeability variations vs time (San Juan)

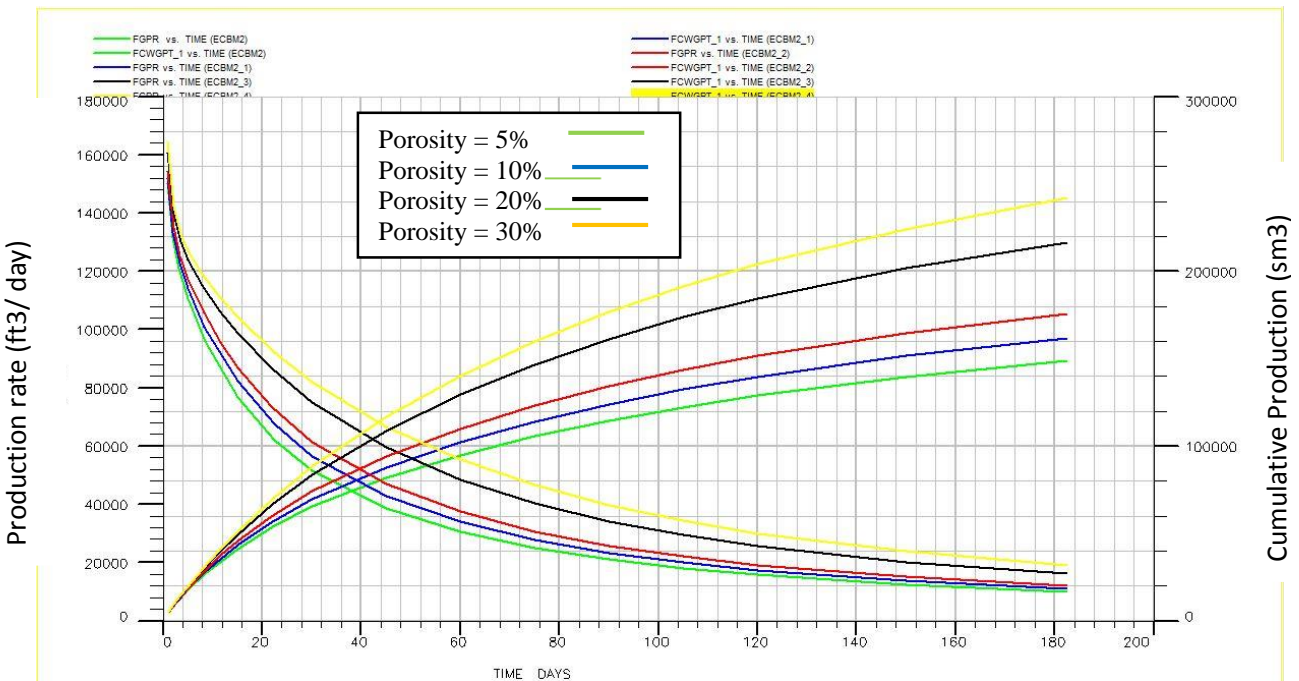


Figure 4.3.4 Field gas production due to porosity variations vs time (San Juan)

Figures 4.3.3 and 4.3.4 show the permeability and porosity simulation results for the San Juan coal basin. Results show that in the initial stage of production, increasing the permeability of the formation will result in a rapid increase of the gas production rate and the cumulative gas production. As production continues, both the gas rate and cumulative production tend to become constant. Furthermore, results in this basin indicate that in the final stages of production the lower values of permeability give higher gas rates compared to the high permeability values. This phenomena can be due to the rapid increase in production rates at the initial stages of production.

On the other hand, the porosity simulation results for the San Juan basin shown in figure 4.3.4, indicate that the gas rate increases from the initial lower porosity to the highest. That is, as the coal porosity is increased from 5% to 10% for example, gas production rate curve will have higher values compared to the initial curve. From the graph, it can be seen that both the field gas production and the cumulative gas production curves never reach constant values throughout the production life time of the coal reservoir.

### Case 3: Sarawak Basin

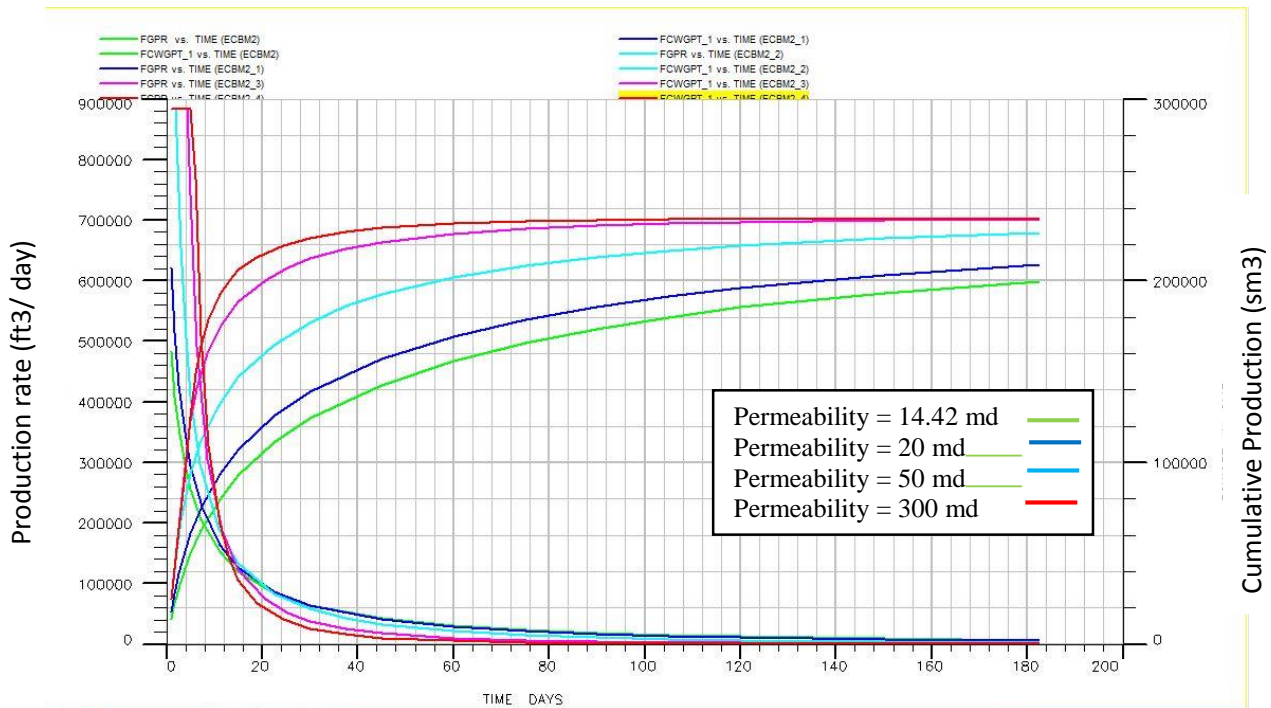


Figure 4.3.5 Field gas production due to permeability variations (Sarawak basin)



Figure 4.3.5 shows the simulation results for the Sarawak coal field due to changes on the initial permeability value. From the figure, it can be observed that as the initial permeability is increased, the gas production rate increases slightly for the first 18 days of production. The gas production and the cumulative gas production tend to become constant as production continues as the reservoir is depleted with time.

**Gas production due to porosity changes:**

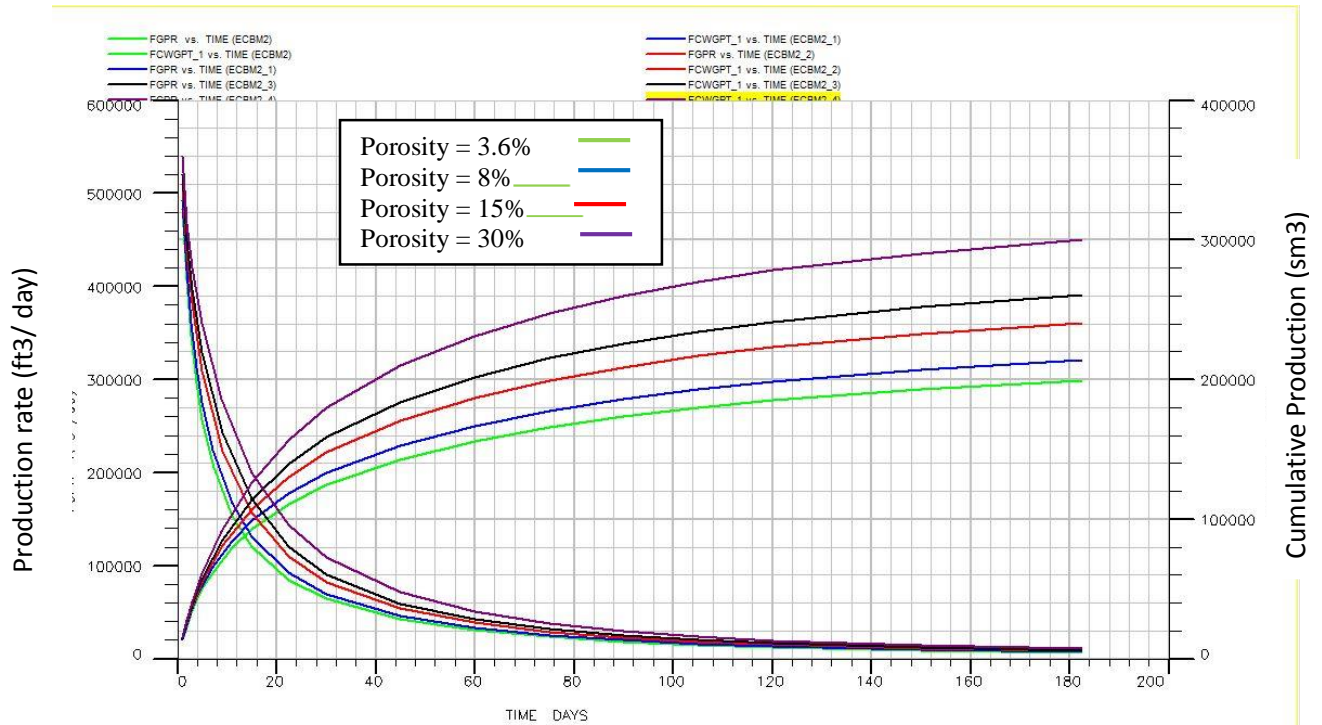


Figure 4.3.6. Field gas production due to porosity variations (Sarawak)

In the figure above, it can be seen that as porosity is increased, the gas production rate and cumulative gas production also increase. This can be observed through analysis of the behavior of the gas rate and cumulative production curves. It can be observed that when porosity is 3.6%, the curves take lower values compared to when the porosity is 8%, 15%, and 30%, respectively.

Table 4.1: Analysis of how much porosity and permeability affects production in all three CBM basins.

| <b>Powder river</b> |                            |               |                     |                            |               |
|---------------------|----------------------------|---------------|---------------------|----------------------------|---------------|
| <b>Porosity</b>     |                            |               | <b>Permeability</b> |                            |               |
| Porosity            | Cumulative production(sm3) | Increment (%) | Permeability        | Cumulative production(sm3) | Increment (%) |
| 0.02                | 223000                     | 0             | 300                 | 217000                     | 0             |
| 0.1                 | 261000                     | 17.04036      | 500                 | 220000                     | 1.382488      |
| 0.18                | 300000                     | 14.94253      | 650                 | 221000                     | 0.454545      |
| 0.25                | 339000                     | 13            | 800                 | 222000                     | 0.452489      |
| <b>San Joan</b>     |                            |               |                     |                            |               |
| <b>Porosity</b>     |                            |               | <b>Permeability</b> |                            |               |
| Porosity            | Cumulative production(sm3) | Increment (%) | Permeability        | Cumulative production(sm3) | Increment (%) |
| 0.05                | 142000                     | 0             | 3.65                | 98000                      | 0             |
| 0.1                 | 160000                     | 12.67606      | 25                  | 200000                     | 104.0816      |
| 0.2                 | 220000                     | 37.5          | 50                  | 225000                     | 12.5          |
| 0.3                 | 240000                     | 9.090909      | 100                 | 228000                     | 1.333333      |
| <b>Sarawak</b>      |                            |               |                     |                            |               |
| <b>Porosity</b>     |                            |               | <b>Permeability</b> |                            |               |
| Porosity            | Cumulative production(sm3) | Increment (%) | Permeability        | Cumulative production(sm3) | Increment (%) |
| 0.036               | 200000                     | 0             | 14.42               | 200000                     | 0             |
| 0.08                | 219000                     | 9.5           | 20                  | 210000                     | 5             |
| 0.15                | 240000                     | 9.589041      | 50                  | 242000                     | 15.2381       |
| 0.3                 | 260000                     | 8.333333      | 300                 | 258000                     | 6.61157       |



Form the table 4.1, it can be observed that as permeability and porosity values are increased (stimulated), the cumulative production of methane also increases. Detailed analysis are presented below:

- **Powder River basin:**

Porosity increases from 2 % to 10%, an increment on the production of methane of about 17% is observed. Moreover, when porosity changes from 10% to 18%, production of methane increases by 15 %. From this observations, it can be concluded that the more porous the coal formation, methane recovery will be higher. The reduction on the percentage of increment is due to the production process. As the reservoir is depleted, the less gas is left in the reservoir compared to the initial stages.

Analysis of permeability on the same basin show an increment of approximately 1.4 % in cumulative production as the permeability is increased from the initial 300 md to 500md. Furthermore, as the coal is stimulated from 500 to 800 md, the cumulative production of methane tends to increase by 0.45%, due to less volume of methane remaining in the reservoir.

- **San Juan basin:**

Observations of the simulation results of San Juan basin indicate that when porosity of the coal is changed from 5% to 10% the cumulative production of methane increases by approximately 12.7% and as it is changed from 10% to 20% methane production increases by 37.5%. At porosity of 30% the production increases by 9%. The sudden decrease on production is related to the initial gas in place.

The production increases by 104% as permeability is stimulated from 3.65 md to 25 md. After that, when permeability is increased from 25 to 50 md and from 50 to 100 md it is observed that the production increment tends to decrease. This is due to the effect of fracture length of the hydraulic fracturing. The fracture propagation reaches a point where the compressive strength of the coal is too high, therefore the effect of the injected fluid is no longer felt.

- **Sarawak basin:**

In the Sarawak basin, as permeability is increased from the initial 14.42 to 20 md, production increases by 5%, and as it is changed to 50 md, production increases by 15%. From these observations, it can be concluded that at the initial stages of production, permeability affects largely on the production rate, compared to the late stages (when the fracture propagation is no longer felt).

The cumulative production increases by 9.5 %, 9.58% and 8.3% as porosity of the coal formation is increased from 3.6% to 8%, 8% to 15%, and from 15% to 30% respectively.

All the production rate curves from the three coal fields show similarities in terms of their behavior. Firstly, the gas production rate due to permeability variations increase very quickly in the initial stages of production. This can be attributed to the instantaneous diffusion of fluids from coal matrix into the fractures of the coal. In other words, the production rate curves in all the basins can be analyzed in three stages: The first stage is the rapid increase on the rate (generally during the first 30 days of production), then at a specific day the production rate becomes the same regardless of the value of permeability. The final stage is characterized by a constant decline in production rate as production continues until e total depletion (zero production rate). The limiting factor is the Langmuir volume, which is the maximum gas content of the coal. The high permeability results is faster production of gas, which in turn results in faster depletion of the gas content, hence resulting in equal production totals of coal reservoirs at a specific permeability value.

The cumulative production curves from the three basins tend to have a rapid increase in the first 30 days of production and become constant as the reservoir is depleted for different values of permeability. For permeability variations, it can be said that when permeability rises, total production also raises.

From the porosity it can be observed that the production curves are never the same. That is, different porosity values produce different production rate and cumulative production curves throughout the life time of the coal field. This is because the larger pore spaces, the rock capacity to accumulate natural gas is also high.

Furthermore, the initial reservoir pressure and Langmuir volume also plays vital roles in the production profile of the fields. The larger the Langmuir volume, the greater capacity for coal storage. However, Langmuir pressure has an adverse effect of gas production. Higher Langmuir pressure means a high pressure is required for the gas to be adsorbed on the internal surface of the coal. Therefore, in coal with high Langmuir pressure, the methane content is less, and hence production rates will deplete much faster.

Understanding all the characteristics of coal formation is important to study the production trends and profiles of each field. However, permeability has the most profound effect in production rates since it is permeability that allows the fluids in the reservoir to flow out, into the wellbore.

## **CHAPTER 5: CONCLUSION AND RECOMENDATIONS**

### **5.1 Conclusions**

Mass transport in CBM fields depends on the methane concentration gradient not the pressure gradient like in the conventional reservoirs. Moreover, two models control the productivity of CBM: the dual porosity model and the dual permeability model. The matrix pores of low rank coal are larger than those of middle and high rank coals, therefore the ratio of free gas is higher in the low coal ranks coal bed methane fields. Moreover, as the coal rank increases, the cleat system also increases and hence the permeability will increase.

Studies indicate that there are various methods that can be used to improve the productivity of a CBM field. Hydraulic fracturing is the process of injecting fluids at high pressure into the formation, causing it to fracture. This method is used in this research in order to simulate changes of permeability and porosity.

In the case of coal, there are five fluids used during the hydraulic fracturing process: water with proppant, water without proppant, nitrogen foam, crosslinked gel and linear polymer.

It has clearly been demonstrated through the literature and simulation conducted in this research that when fluid is injected (hydraulic fracturing) to the coal at various pressures and rates coal seam physical properties such as permeability and porosity can be improved.

The resultant improvement of porosity and permeability by hydraulic fracturing can affect the production behavior of the coal fields. Permeability and porosity simulation results from three coal fields (Powder River, San Juan and Sarawak) indicate that both the gas production rate as well as the cumulative production are increased as the permeability and porosity are changed from low to high values. The rapid increase of production rate in the early time of production can be related to the fast diffusion of fluids from coal matrix into the fractures of the coal. Finally the total gas production depends also on the Langmuir volume of the coal.

## **5.2 Recommendations**

It is recommended that further research in the coal geological properties should be conducted in order to clearly understand their impact in production. Secondly coal geo-mechanics must be analyzed thoroughly so that hydraulic fracturing impact can be maximized. The understanding of the above mentioned properties will enable a much more clear understanding and interpretation of the fluid flow mechanisms governing coal formations, hence contributing to higher methane gas recovery from coals.

On the other hand it is recommended that the project time should be increased in order to run more simulations and obtain much more accurate results. In addition, reliable and complete data sources should be provided in future in order to eliminate many assumptions. Lab equipment and facilities should as well be properly equipped and fully functional so that project time can be entirely dedicated to relevant tasks.

More studies should be conducted in the production optimization of CBM focusing on the influence of permeability and porosity and resources should adequately be allocated into CBM optimization because CBM has proven to be one of the future next power generation sources.

## References

- Abass, H. H., Kim, C. M., & Hedayati, S. (1991). *Experimental Simulation of Hydraulic Fracturing In Shallow Coal Seams*.
- Barr, K. L. (2009). *A Guideline to Optimize Drilling Fluids for Coalbed Methane Reservoirs*.
- Chaianansutcharit, T., Chen, H.-Y., & Teufel, L. W. (2001). *Impacts of Permeability Anisotropy and Pressure Interference on Coalbed Methane (CBM) Production*.
- Chase, R. W. (1977). *Natural Gas Production From Coal Seams*.
- Chen, D., Liu, J., Pan, Z., & Connell, L. *Coalbed Methane Production: Why Coal Permeability Matters*.
- Chen, Z., Liu, J., Kabir, A., Wang, J., & Pan, Z. (2013). Impact of Various Parameters on the Production of Coalbed Methane. doi: 10.2118/162722-PA
- Connell, L., & Lu, M. (2007). A dual-porosity model for gas reservoir flow incorporating adsorption behaviour—Part II. Numerical algorithm and example applications. *Transport in porous media*, 69(2), 139-158. doi: 10.1007/s11242-007-9140-5
- Djebbar Tiab, E. C. D. (2004). *Petrophysics: Theory and Practice of Measuring Reservoir Rock and Fluid Transport Properties* (Second ed.). Linacre House, USA: Elsevier.
- Dong, Z., Holditch, S. A., Ayers, W. B., & Lee, W. J. *Probabilistic Estimate of Global Coalbed Methane Recoverable Resources*.
- Haimson, B., & Fairhurst, C. (1969). Hydraulic Fracturing in Porous-Permeable Materials. doi: 10.2118/2354-PA
- Hassim, A. H. R. B. (2012). *The Effect of Permeability towards Coalbed Methane (CBM) Production*. (Final Year Project), Universiti Teknologi Petronas, Tronoh, Perak. Retrieved from <http://utpedia.utp.edu.my/id/eprint/5678>
- Hoyer, D. L. (1991). Evaluation Of Coalbed Fracture Porosity From Dual Laterolog.
- Jikich, S. A., McLendon, R. T., & Smith, D. H. *Permeability Variations in Upper Freeport Coal Cores Due to Changes in Effective Stress and Sorption*.
- Jochen, V. A., & Lee, W. J. (1994). *Determining Permeability in Coalbed Methane Reservoirs*.
- Jon Gluyas, R. S. (2004). *Petroleum Geoscience*.

- Keshavarz, A., Khanna, A., Hughes, T., Boniciolli, M., Cooper, A., & Bedrikovetsky, P. (2014). *Mathematical Model for Stimulation of CBM Reservoirs During Graded Proppant Injection*.
- Materials, A. S. f. T. a. (1998). Standard Classification of Coal by Rank. Washington, DC, United States of America.
- Mavko, B. B., Hanson, M. E., Nielsen, P. E., & Logan, T. L. (1986). *Hydraulic Fracture Model For Application To Coal Seams*.
- Purl, R., Evanoff, J. C., & Brugler, M. L. (1991). *Measurement of Coal Cleat Porosity and Relative Permeability Characteristics*.
- Ramachandran, R., & Shirley, A. I. (1994). Method of recovery of natural gases from underground coal formations: Google Patents.
- Ren, W., Wang, H., Shi, J., Sun, F., Li, Y., Wang, Z., . . . Xu, Z. (2013). *Desorption And Transport Mechanisms Of Gas Through Coal Matrix Pores And Gas Production Forecasting*.
- Wikipedia. (2010). Coalbed Methane *Coalbed methane*.
- Wu, Y., Liu, J., & Elsworth, D. *Development of Permeability Anisotropy During Coalbed Methane Production*.

## Appendix A

Table : Coal matrix pores classification table by various authors.

Source: (Ren et al.).

| Xont (1961)                     | Dubin (1966)               | Gan (1972)                  | IUPAC (1978) Fushun       | Coal Institute (1985)      | Jun We (1991)                 | Sijing Yang (1991)            | Xuehai Fu (2005)                |
|---------------------------------|----------------------------|-----------------------------|---------------------------|----------------------------|-------------------------------|-------------------------------|---------------------------------|
| Mirco pores, < 10 nm            | Mirco pores, < 2 nm        | Micro pores, < 1.2 nm       | Micro pores, < 2 nm       | Micro pores, < 8 nm        | Micro pores, < 5 nm           | Micro pore, < 10nm            | Micro pores, <8 nm              |
| Transition pores, 10 -00 nm     | Transition pores, 2- 20 nm | Transition pores, 1.2-30 nm | Transition pores, 2-50 nm | Transition pores, 8-100 nm | Transition pores, 5-50 nm     | Transition pores, 10-50 nm    | Transition pores, 8-20 nm       |
| Intermediate pores, 100-1000 nm |                            |                             |                           |                            | Intermediate pores, 50-500 nm |                               | Intermediate pores, 50 – 750 nm |
|                                 |                            |                             |                           |                            |                               | Intermediate pores, 65-325 nm |                                 |
| Macro pores, > 1000 nm          | Macro pores, >20 nm        | Macro pores, > 1000 nm      | Macro pores, >50nm        | Macro pores, > 100 nm      | Macro pores, 500-750          | Macro pores, > 1000 nm        | Transition pores, 325-1000 nm   |
|                                 |                            |                             |                           |                            |                               |                               | Micro pores, >1000 nm           |



**Appendix B:**

Table of base case coal properties of Powder River Basin, San Juan and Sarawak.

( source:(Hassim (2012)))

| <b>Properties</b>                 | <b>Powder River Basin</b>              | <b>San Juan Basin</b>                  | <b>Sarawak</b>                         |
|-----------------------------------|--|--|--|
| Coal thickness (h)                | 64ft                                   | 29.527ft                               | 24.25ft                                |
| Top of coal                       | 557ft                                  | 4112.8ft                               | 660ft                                  |
| Initial Permeability (Ko)         | 300 md                                 | 3.65md                                 | 14.42md                                |
| Initial Porosity ( $\phi_0$ )     | 2%                                     | 5.0%                                   | 3.6%                                   |
| Coal compressibility (Cf)         | $1.0 \times 10^{-6} \text{ psia}^{-1}$ | $1.0 \times 10^{-6} \text{ psia}^{-1}$ | $1.0 \times 10^{-6} \text{ psia}^{-1}$ |
| Reservoir temperature (T)         | 65 F                                   | 113 F                                  | 75 F                                   |
| Initial reservoir pressure (Pres) | 152.5 psia                             | 1109.5 psia                            | 200 psia                               |
| Water saturation (Sw)             | 50%                                    | 59.2%                                  | 50%                                    |
| Coal Density                      | 83.34lb/ft <sup>3</sup>                | 89.5lb/ft <sup>3</sup>                 | 83.34 lb/ft <sup>3</sup>               |
| Coal moisture content             | 27.49%                                 | 6.72%                                  | 23.25%                                 |
| Coal ash content                  | 4.40%                                  | 14.6%                                  | 5.95%                                  |
| Langmuir Pressure (Pl)            | 394 psia                               | 4688.5 psia                            | 1024 psia                              |
| Langmuir Volume (Vl)              | 116.8 scf/ton                          | 486 scf/ton                            | 714.29 scf/ton                         |